

JOURNAL REVIEW

Simulation of Buoyancy Driven Bubbly Flow: Established Simplifications and Open Questions

A. Sokolichin and G. Eigenberger

Institut für Chemische Verfahrenstechnik, Universität Stuttgart, D-70199 Stuttgart, Germany

A. Lapin

Institut für Bioverfahrenstechnik, Universität Stuttgart, D-70569 Stuttgart, Germany

An assessment is given of the present state of modeling and simulation of buoyancy driven gas-liquid bubble flow based on the two-fluid approach. Main points of discussion comprise the admissible model simplifications in order to obtain a more easily solvable model together with the question of which physical effects are of prime importance and which reliable correlations can be recommended or are still missing. It is shown that, for most practical cases, the two-fluid model can be simplified to a formulation which allows for the application of efficient solution strategies for single-phase flow. From the different interaction forces between gas and liquid, pressure and drag force are most important, whereas no sound experimental basis is available for (lateral) lift forces. So far, lift forces have primarily been used empirically to adjust the gas distribution to the experimental observation. The main open question concerns the proper modeling of turbulence in gas-liquid bubble flow since it affects both the mixture viscosity and the bubble dispersion.

© 2004 American Institute of Chemical Engineers *AIChE J*, 50: 24–45, 2004

Keywords: modeling, simulation, gas-liquid flow, bubbly flow, bubble induced turbulence, fluid dynamics

Introduction

Bubble induced gas-liquid flow is the basis of fluid movement in many chemical engineering devices and applications ranging from boilers or evaporators over two- or three-phase bubble column reactors of various design to large-scale aerobic (and sometimes anaerobic) sewage treatment plants. About 10 years ago, modeling and simulation of these systems was restricted to strongly simplified (overall) fluid-flow models, primarily because the computer power for the solution of more detailed models was not sufficient. In the meantime a number of efficient commercial CFD-codes are available and the power of desktop PC or workstations is

strong enough for quite detailed simulation studies (Sanyal et al., 1999; Krishna et al., 2000; Pflieger and Becker, 2001). In most cases reasonable to good agreement of experimental results and simulations has been shown or claimed, implying that the predictive power of CFD simulations for bubble flow is already at a reliable level. A closer look, however, reveals that the question of which physical effects are of prime importance and how they should be modeled is still under strong debate.

In this contribution we therefore try to assess the generally accepted and/or well documented state of bubble flow modeling and point at the questions which are unresolved or under dispute. The discussion will be restricted to buoyancy driven bubble flow excluding forced convection. It will only consider the volume averaged two-fluid approach, which presently seems best suited for a simulation of larger-scale systems.

Correspondence concerning this article should be addressed to A. Sokolichin at alexcde@icvt.uni-stuttgart.de.

G. Eigenberger's e-mail address is eigenberger@icvt.uni-stuttgart.de.

The last comprehensive reviews on the modeling of bubble driven flows were Jakobsen et al. (1997), Joshi (2001), Joshi et al. (2002). They listed the different approaches for the modeling of bubble-liquid interaction forces and only briefly addressed bubble induced turbulence. Joshi (2001) also clearly pointed at the large number of unresolved questions and gave suggestions for future work. In this contribution we want to answer some of these questions like the influence of the numerical solution procedure, the necessity of a three-dimensional (3-D), fully dynamic simulation for most applications, and the importance of different modeling assumptions for gas-liquid interaction, while stressing the still unknown or unresolved points. We will critically evaluate the different modeling aspects with respect to their influence on simulation results in the above specified range of operating conditions, as well as their present state of experimentally approved justification.

Two-Fluid Euler-Euler Model

The derivation of the model equations for the two-phase bubbly flow starts with the assumption that both phases can be described as continua, governed by the partial differential equations of continuum mechanics. The phases are separated by an interface, which is assumed to be a surface. At the interface, jump conditions for the conservation of mass and momentum can be formulated (Ishii, 1975; Drew, 1983).

The direct solution of these microscopic equations supplemented by appropriate initial conditions would yield a complete description of the two-phase flow. This approach is called direct numerical simulation (DNS). Since systems of practical interest usually comprise a large number of interacting bubbles, such problems are far too complicated to permit a direct solution. The application of DNS to the simulation of turbulent two-phase flow is thus restricted to the flow around a few gas bubbles (Lin et al., 1996; Tryggvason et al., 1998) and cannot be used for modeling of industrial-scale reactors.

The problem has to be simplified by replacing the point variables by variables averaged over space and/or time. The resulting equations describe the motion of the two phases (fluids) as if they were interpenetrating and interacting continua, assuming that each element or finite volume of the spatial domain contains a certain fraction ε_l of the continuous (liquid) and a fraction $\varepsilon_g = 1 - \varepsilon_l$ of the dispersed (gas) phase. Since the resulting equations are formulated in the Eulerian frame of reference, such models are called two-fluid or Euler-Euler models.

The simplified viewpoint provided by the two-fluid models requires the specification of phase forces and of stress terms in the momentum equations (the latter are often called *turbulent* stress terms, although they have a somewhat different origin). The form of these "closure" terms has to be determined empirically or even postulated. This gives room for controversy with respect to the final form of the macroscopic equations describing bubbly flow.

However, apart from the differences in the modeling of the interphase force and the turbulence terms, most of the two-fluid models presented in the literature are very similar to each other and consist of the continuity and momentum equations for the gas phase (index g) and the liquid phase (index l). If the discussion is restricted to bubble flow hydrodynamics, the following additional assumptions are usually made: isothermal

conditions; no mass transfer between the two phases; constant liquid density ρ_l ; gas density ρ_g depending on local pressure p as described by the ideal gas law; and all bubbles generated at the sparger are grouped into bubble classes of constant mass; the bubbles of each class retain their mass as long as they are in the two-phase flow domain. This means that: bubble coalescence and re-dispersion are neglected.

These assumptions will also be used in the following.

Continuity equations

Since no mass transfer is considered between gas and liquid, the continuity equation can be formulated for both phases independently without an additional mass-transfer term

$$\frac{\partial(\varepsilon_k \rho_k)}{\partial t} + \nabla \cdot (\varepsilon_k \rho_k \mathbf{u}_k) = 0 \quad k = l, g \quad (1)$$

Momentum balances

Since molecular viscous stress tensor can be neglected in comparison with the turbulent stress tensor for both phases, the momentum balances can be formulated according to Drew (1983) as

$$\begin{aligned} \frac{\partial(\varepsilon_k \rho_k \mathbf{u}_k)}{\partial t} + \nabla \cdot (\varepsilon_k \rho_k \mathbf{u}_k \mathbf{u}_k) \\ = \nabla \cdot \varepsilon_k \mathbf{T}_k^{\text{turb}} - \varepsilon_k \nabla p + \varepsilon_k \rho_k \mathbf{g} \pm \mathbf{F}_{\text{int}} \quad k = l, g \end{aligned} \quad (2)$$

The only difference between the momentum equations for the two phases is the sign of the interaction force \mathbf{F}_{int} , which is positive for the liquid phase and negative for the gas phase. The first term on the righthand side corresponds to the momentum flux due to turbulent stresses, which can be evaluated from an appropriate turbulence model. The modeling of the interaction force \mathbf{F}_{int} and of the turbulent stresses will be discussed in subsequent sections. At this stage, it is assumed that these terms are known.

If bubbles of different mass have to be considered, separate continuity equations and momentum balances are required for each bubble class.

Invoking the equations of state for each phase

$$\rho_l = \text{const} \quad (3)$$

$$\rho_g = \frac{p}{RT_o} \quad (4)$$

and the closure relation

$$\varepsilon_l + \varepsilon_g = 1 \quad (5)$$

we obtain a closed system of differential and algebraic equations, which describes the dynamic behavior of the two-phase flow and can be solved numerically.

Model Simplifications and Numerical Solution Procedure

Detailed comparison between experiments and simulations has shown that important characteristics of the flow structure can only be resolved by a 3-D dynamic simulation on a sufficiently fine spatial grid (Sokolichin and Eigenberger, 1999; Borchers et al., 1999). It is obvious that an accurate integration in time is equally important. Since the dynamic solutions have to be computed on fine spatial grids over a prolonged real-time period, the availability of efficient numerical solution procedure is of decisive importance.

Before discussing the modeling of the interphase force F_{int} and of the turbulent stresses T_k^{turb} , we will therefore discuss the two-fluid model (1–5) from the numerical point of view.

The numerical load depends on the number and the complexity of the different terms in the model equations and on the rate of convergence of the iteration loops which, in turn, depends on the number and the character of the coupling terms between the model equations. Model simplifications are, therefore, essential for an increased speed of convergence.

The influence of the different model simplifications on the accuracy of the solution in specific situations is at present not sufficiently understood. Its systematic investigation presents an important direction for further research. In the following, some crucial model assumptions and simplifications will be described and their implications—as far as presently known—will be discussed.

Pressure equation

The set of equations describing the hydrodynamics in a gas-liquid system can only be solved effectively if it is possible to decouple the solution procedure so that an efficient iterative scheme can be used. Since the model contains no explicit equation for the determination of the pressure, Patankar (1980) derives such an expression for a single-phase system through a transformation of the continuity equation. In a two-phase system the derivation of a respective equation is more complicated than in the single-phase case, because two continuity equations have to be considered instead of one (Spalding, 1985). The resulting pressure equation is no longer linear, but quadratic and requires additional iterations.

At low gas holdups, the value of ε_l is close to one. If we neglect the variation of ε_l due to the presence of gas in the continuity equation of the liquid phase

$$\frac{\partial \varepsilon_l}{\partial t} + \nabla \cdot (\varepsilon_l \mathbf{u}_l) = 0 \quad (6)$$

it will be transformed into

$$\nabla \cdot \mathbf{u}_l = 0 \quad (7)$$

This allows to derive a pressure equation as in the single-phase case. The continuity equation of the gas phase can then be used to calculate the local gas holdup distribution.

Let us study the validity of this simplification in the case when the gas holdup is *not* very close to zero. If we assume both phases to be incompressible, we can eliminate the densi-

ties from the continuity equations, and the sum of the continuity equations for both phases results in

$$\nabla \cdot (\varepsilon_l \mathbf{u}_l + \varepsilon_g \mathbf{u}_g) = 0 \Leftrightarrow \nabla \cdot \mathbf{u}_l + \nabla \cdot [\varepsilon_g (\mathbf{u}_g - \mathbf{u}_l)] = 0 \quad (8)$$

Since the slip velocity $\mathbf{u}_{\text{slip}} = (\mathbf{u}_g - \mathbf{u}_l)$ is dominated by the vertical component u_{slip}^x and is approximately constant, Eq. 8 implies that

$$\nabla \cdot \mathbf{u}_l \approx -u_{\text{slip}}^x \frac{\partial \varepsilon_g}{\partial x} \quad (9)$$

We see that, even at higher gas holdups, Eq. 7 is a good approximation to Eq. 9, if the gas holdup does not vary too much in the vertical direction. This condition is, of course, violated during the first seconds after the onset of the aeration, when the gas front propagating through the reactor has a sharp discontinuity in the vertical direction. As long as the gas front has not reached the free surface, the integral gas holdup in the reactor increases continuously leading to the rise of the free surface. If Eq. 7 is used instead of Eq. 6, this effect cannot be reproduced in the simulation. Figure 1 shows the liquid velocity field and the gas holdup 0.1 s after the onset of the aeration in a 2-D locally aerated flat bubble column (see Becker et al. (1994) for the description of the test case). The simulation results obtained with Eq. 6 show that the liquid velocity has a positive vertical component almost everywhere in the column, because the liquid is displaced by the rising gas (Figure 1, left). Equation 7 neglects this displacement effect, and the motion in the liquid phase can be observed only in the vicinity of the sparger (Figure 1, right), due to the density differences in the gas/liquid-mixture (the buoyancy effect).

After the gas front has reached the liquid surface, the integral gas holdup in the reactor does not increase anymore and the level of the free surface remains approximately constant. The distribution of the gas holdup no longer has sharp discontinuities in the vertical direction, so that Eq. 7 is a good approximation to Eq. 9 and can be used instead of Eq. 6 for the derivation of the pressure equation. Figure 2 presents the simulation results 10 s after the onset of the aeration. We see that now the liquid velocity field and the gas holdup distribution calculated with either Eq. 6 or Eq. 7 agree almost completely.

Momentum balance for the gas/liquid mixture

In the last subsection we discussed the volumetric coupling between the two phases. This coupling effect stems from the fact that each change of the volume fraction of the gas phase requires a respective change in the liquid phase. We have seen that this coupling effect can be neglected under quite realistic conditions.

The other—much more important—coupling mechanism between the liquid and the gas phase manifests itself in the presence of the interaction force term F_{int} in both momentum balances of the two-fluid model. On the one hand, the motion of the bubbles is affected by the flow of the surrounding liquid. On the other hand, the liquid phase is accelerated by the bubbles, which are ascending relative to the surrounding liquid. The two-fluid model takes both effects into account by means

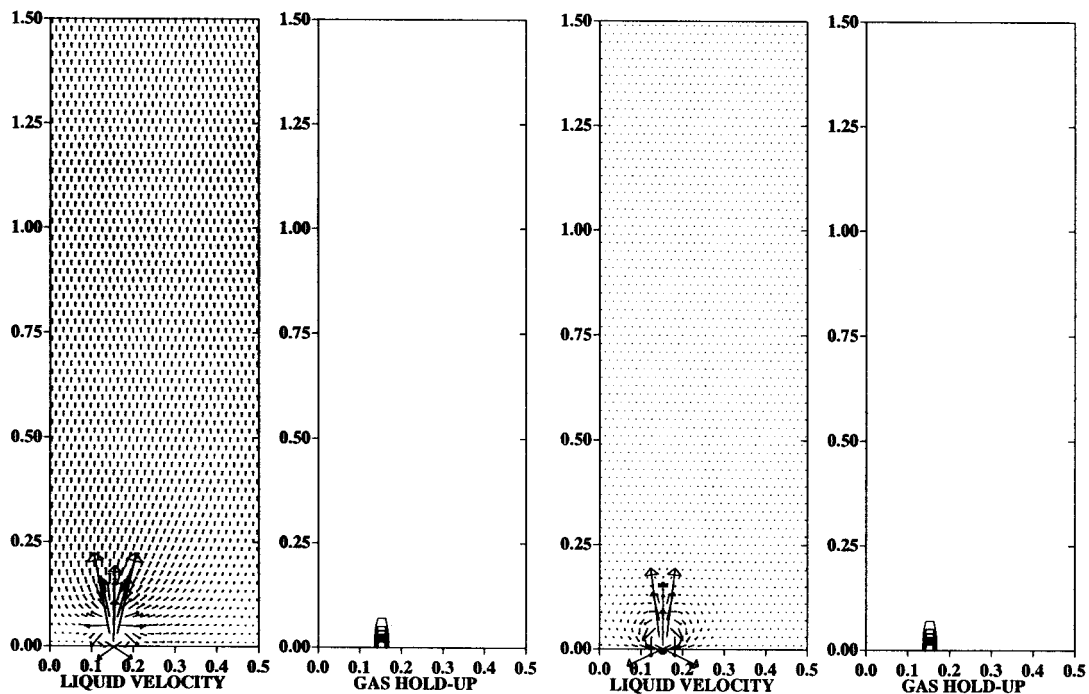


Figure 1. Locally aerated flat bubble column.

Liquid velocity field and the distribution of the gas holdup 0.1 s after the onset of the aeration calculated using Eq. 6 (left) and Eq. 7 (right). (2-D-simulation with laminar viscosity.)

of the interphase force terms in the momentum balances, so that one speaks of the two-way coupling mechanism.

In the iterative numerical solution, the consideration of the full two-way coupling leads to severe convergence problems, if

the momentum equations for both phases are solved independently. One possible way to overcome these difficulties is to omit the interaction force from the momentum balance for the liquid phase, neglecting the influence of the dispersed phase on

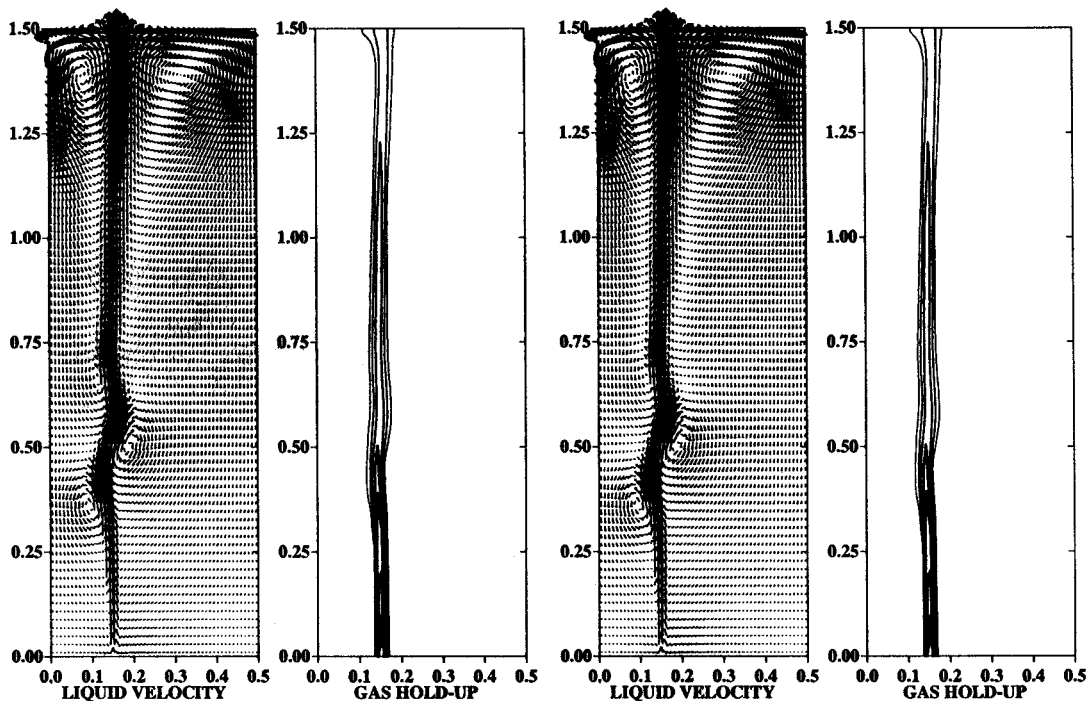


Figure 2. Same example as Figure 1, 10 s after the beginning of the aeration, calculated with Eq. 6 (left) and Eq. 7 (right). (2-D-simulation with laminar viscosity.)

the motion of the continuous phase. This means that the mathematical model provides for the one-way coupling only. The restriction to the one-way coupling is admissible only in cases when the liquid phase is driven mechanically, and the volume fractions of the dispersed phase are very moderate.

However, in the case of bubble columns and airlift loop reactors, the fluid motion is induced by density differences between the aerated and nonaerated regions. This buoyancy effect can only be reproduced if the full two-way coupling is considered. In case of the one-way coupling, the gas bubbles would be moving upwards through the reactor without affecting the liquid phase, as shown by Delnoij et al. (1997a, Figure 9).

A better way to accelerate the convergence of the numerical algorithm is to rearrange the model equations in such a way that the coupling between the resulting equations becomes weaker than in the original system. Such rearrangement can be done either on the level of the *discretized* equations (as in the partial elimination algorithm (PEA), proposed by Spalding (1976)) or on the level of *differential* equations. Our experience shows that in the case of bubbly flows the second approach is much more effective. Since this approach is still not generally accepted by the CFD community, we will describe it in some detail.

First, we replace the momentum balance for the liquid phase by the momentum balance for the gas-liquid mixture by adding the momentum balances (2) for both phases

$$\frac{\partial(\varepsilon_l \rho_l \mathbf{u}_l)}{\partial t} + \nabla \cdot (\varepsilon_l \rho_l \mathbf{u}_l \mathbf{u}_l) + \frac{\partial(\varepsilon_g \rho_g \mathbf{u}_g)}{\partial t} + \nabla \cdot (\varepsilon_g \rho_g \mathbf{u}_g \mathbf{u}_g) = \nabla \cdot \varepsilon_l \mathbf{T}_l^{\text{turb}} + \nabla \cdot \varepsilon_g \mathbf{T}_g^{\text{turb}} - \nabla p + \varepsilon_l \rho_l \mathbf{g} + \varepsilon_g \rho_g \mathbf{g} \quad (10)$$

The important advantage of this equation is that it does not contain the interphase force \mathbf{F}_{int} . Different from the one-way coupling model, the interaction force \mathbf{F}_{int} was not neglected but is canceled out as a result of a mathematical transformation. Thus, the buoyancy effect is still reproduced by the mathematical model, as we will see later.

The momentum balance for the gas-liquid mixture now contains more terms than the momentum balance for the liquid phase. In case of general two-phase flow, there is no advantage of solving the mixture momentum balance instead of the momentum balance for the continuous phase. However, in the case of a gas/liquid bubbly flow, we can use the fact that the density of the gas phase is usually much smaller than the density of the liquid phase and omit the terms containing ρ_g without great loss of accuracy. We obtain (note that T_k^{turb} is proportional to ρ_k , as shown by van den Akker (1986))

$$\frac{\partial(\varepsilon_l \rho_l \mathbf{u}_l)}{\partial t} + \nabla \cdot (\varepsilon_l \rho_l \mathbf{u}_l \mathbf{u}_l) = \nabla \cdot \varepsilon_l \mathbf{T}^{\text{turb}} - \nabla p + \varepsilon_l \rho_l \mathbf{g} \quad (11)$$

This is numerically a much more convenient form, as we will see in the following section.

To make the similarities between single-phase flow and two-phase bubble flow more obvious, we will introduce a further simplification, which represents the limiting case of sufficiently small local gas holdup ε_g . We can then assume the value of $\varepsilon_l = 1 - \varepsilon_g$ to be equal to unity in all terms except for the gravity force, yielding

$$\frac{\partial(\rho_l \mathbf{u}_l)}{\partial t} + \nabla \cdot (\rho_l \mathbf{u}_l \mathbf{u}_l) = \nabla \cdot \mathbf{T}_l^{\text{turb}} - \nabla p + \rho_l \mathbf{g} - \varepsilon_g \rho_l \mathbf{g} \quad (12)$$

This simplification resembles the Boussinesq approximation (Boussinesq, 1903) frequently employed in the modeling of free convection in single-phase systems, where the variation of density due to temperature gradients is considered only in the gravity term, whereas all other terms in the Navier-Stokes equations coincide with those for an incompressible fluid.

Numerical solution

After the simplification described in the previous subsection, the resulting system of model equations for bubble flow with small gas holdup reads

$$\nabla \cdot \mathbf{u}_l = 0 \quad (13)$$

$$\frac{\partial(\rho_l \mathbf{u}_l)}{\partial t} + \nabla \cdot (\rho_l \mathbf{u}_l \mathbf{u}_l) = \nabla \cdot \mathbf{T}_l^{\text{turb}} - \nabla p + \rho_l \mathbf{g} - \varepsilon_g \rho_l \mathbf{g} \quad (14)$$

$$\rho_l = \text{const} \quad (15)$$

$$\begin{aligned} \frac{\partial(\varepsilon_g \rho_g \mathbf{u}_g)}{\partial t} + \nabla \cdot (\varepsilon_g \rho_g \mathbf{u}_g \mathbf{u}_g) \\ = \nabla \cdot \varepsilon_g \mathbf{T}_g^{\text{turb}} - \varepsilon_g \nabla p + \varepsilon_g \rho_g \mathbf{g} - \mathbf{F}_{\text{int}} \end{aligned} \quad (16)$$

$$\rho_g = \frac{p}{RT_o} \quad (17)$$

$$\frac{\partial(\varepsilon_g \rho_g)}{\partial t} + \nabla \cdot (\varepsilon_g \rho_g \mathbf{u}_g) = 0 \quad (18)$$

Equations 13–15 fully correspond with the mass and momentum balance equations and the equation of state for **one-phase** flow, except for the last term on the righthand side of Eq. 14. This term describes a force which is directed upwards and is proportional to the local gas holdup. The gas-liquid flow can thus be interpreted as a one-phase flow with an additional buoyancy source term in the momentum balance. This means that the first three equations can be solved in exactly the same way as in the one-phase case using some iteration procedure, for example, the SIMPLER scheme of Patankar (1980). The only modification of this algorithm is that at the end of each iteration loop we have to update the local values of ε_g in the spatial domain. The sequence of operations can be summarized as follows:

- (1) Start with the liquid velocity, pressure and gas holdup values from the end of the last time step.
- (2) Calculate the new liquid velocity field and the new pressure using one iteration of the SIMPLER procedure as described in Patankar (1980).
- (3) Calculate the gas velocity using Eq. 16.
- (4) Calculate the gas density using Eq. 17.
- (5) Solve the gas transport equation (Eq. 18) to obtain the new values of gas holdup.

(6) Return to step 2 and repeat until convergence, then go to the next time step.

The described solution procedure turned out to be very efficient. In most test cases studied so far no underrelaxation was necessary and the convergence could usually be reached after 2–3 iterations, if the time step size was appropriately chosen. The pressure equation and the pressure correction equations were solved using an inner iteration procedure, whereby the best convergence rate was reached using the SIP-method of Stone (1968) or modifications thereof for the 3-D case. As a result, dynamic simulations with a final spatial grid (order of 500,000 grid points) can be performed on standard workstations. A number of numerical examples can be found in Sokolichin and Eigenberger (1999), Borchers et al. (1999), and in this contribution.

The simplified version of the mixture momentum balance (Eq. 12 or 14) was used above in order to make the analogy with the one-phase Navier-Stokes system more evident. If the local gas holdup is not very low, Eq. 11 can be used instead. The values of the liquid holdup needed for solution of Eq. 11 have to be calculated from the relation $\varepsilon_l = 1 - \varepsilon_g$ after performing step 5, which has no influence on the convergence rate of the iteration.

Accuracy of the numerical solution

For many of the numerical simulation results of gas-liquid flows, published in recent years, the influence of the spatial grid resolution and, for dynamic simulations, of the time step size has not obtained the necessary attention.

Our results show that, for first-order methods, the effect of numerical diffusion on the solution accuracy can be devastating (see, for example, Sokolichin et al., 1997). In this respect the very popular *linear* methods using a blending or switching strategy between first- and second-order accurate methods (the well-known “hybrid” and “power-law” schemes, see Patankar (1980)) have to be considered as first-order methods, since in the case of vanishing diffusion coefficients they become equivalent to the first-order upwind scheme. Based upon this experience, we recommend to use the second-order central-difference flux approximation for the diffusive terms and the TVD approach, described in detail by Sokolichin et al. (1997) and Sokolichin and Eigenberger (1999) for all convective terms. The TVD method used is based on a *nonlinear* blending strategy between first and second-order accurate schemes. The computational cost of a TVD scheme (per grid point) is higher than that of first-order schemes, but its computational efficiency (accuracy per overall costs) is much greater, because the TVD discretization is nearly second-order accurate for smooth solutions.

For the time discretization, a fully implicit backward difference time stepping procedure with constant time steps in the range 0.05–0.2 s has been adopted for stability reasons. The use of this first-order accurate scheme is sufficient for the examples presented here, because the flow patterns in the airlift loop reactors are quasi-steady state and the oscillation frequency of the bubble swarm in the locally aerated bubble column is very low, as compared to the time step used in the computations. However, a more refined time step control strategy could certainly increase the efficiency of the computations further.

For all results presented in this article, solutions over a wide range of spatial resolutions and time steps were examined in order to verify the grid independence or at least the grid convergence of the simulation results.

Modeling of the Gas Velocity

In the framework of the two-fluid model (1–5), the interaction force F_{int} appears in the momentum balances for both phases. Since we replaced the momentum balance for the liquid phase by the momentum balance for the gas/liquid mixture, the resulting system (13–18) contains this term only in the momentum balance for the gas phase (16). During the iteration procedure described above, the momentum balance for the gas phase is used for the calculation of the gas velocity.

Instead of modeling the interaction force F_{int} explicitly, a direct way to calculate the velocity of the gas phase can be applied. It is based upon the equation of motion of a single gas bubble in the Lagrangian frame of reference. In a second step (Eq. 44) the velocity of a single bubble u_b can be related to the gas phase velocity u_g .

The motion of gas bubbles can be generally described by Newton’s law

$$\frac{d(m_b u_b)}{dt} = F_{\text{total}} \quad (19)$$

u_b denotes here the Lagrangian velocity of each bubble, m_b is the mass of the bubble, and F_{total} is the sum of all (interfacial and body) forces acting on the bubble. The following forces are usually considered in the literature.

Pressure Force

The pressure force results from the global pressure gradient and can be expressed as

$$F_p = -V_b \cdot \nabla p, \quad (20)$$

where V_b stands for the volume of a single bubble. The pressure force coincides with the Archimedes’ buoyancy force acting on a bubble under the assumption that the actual pressure gradient can be approximated by the hydrostatic pressure gradient $\nabla p \approx \rho_l g$

$$F_p \approx -V_b \rho_l g \quad (21)$$

Gravity Force

The influence of the gravity force can be described by

$$F_g = m_b \cdot g \quad (22)$$

Interaction Forces

Only pressure and gravity forces are acting on a motionless bubble in a liquid at rest. Since there is usually a relative motion between the bubble and the liquid, the liquid flow around individual bubbles leads to local variations in the pressure and shear stress. The resulting interaction forces due to these variations cannot be considered in detail within the

framework of a two-fluid model, but have to be approximated through more or less empirical correlations. Usually three different contributions are taken into account, the drag force F_d , the added mass force F_{am} , and the lift force F_l . The three contributions will be discussed in the following subsections.

Drag Force

A bubble that moves relative to a liquid accelerates part of the liquid around it and is in turn slowed down by the surrounding liquid. This drag force is the dominant contribution to the interaction force and often it is the only one considered. It is common to describe the drag force F_d by

$$F_d = -\frac{1}{2} C_d \rho_l \pi \frac{d_b^2}{4} |\mathbf{u}_b - \mathbf{u}_l| (\mathbf{u}_b - \mathbf{u}_l) \quad (23)$$

d_b denotes here the (equivalent) bubble diameter, and C_d is a (dimensionless) drag coefficient. In the case of single bubbles, C_d has to depend on the bubble Reynolds number (Re), Eötvös number ($E\ddot{o}$), and Morton number (Mo) or Weber number (We) (Clift et al., 1978), which are defined as follows (we assume here that $\rho_g \ll \rho_l$ and use ρ_l instead of $\Delta\rho$)

$$Re = \frac{\rho_l d_b |\mathbf{u}_b - \mathbf{u}_l|}{\mu_l}$$

$$E\ddot{o} = \frac{g \rho_l d_b^2}{\sigma}$$

$$Mo = \frac{g \mu_l^4}{\rho_l \sigma^3}$$

$$We = \frac{\rho_l |\mathbf{u}_b - \mathbf{u}_l|^2 d_b}{\sigma}$$

σ stands for the surface tension coefficient ($\sigma \approx 0.07 \text{ kg/s}^2$ for water). The following discussion of different formulae for the drag coefficient is restricted to the air/water system, since most gas-liquid simulations presented in the literature are dealing with these substances.

The derivation of reliable empirical correlations for the drag coefficient C_d is complicated by the fact that a direct measurement of the drag force acting on a gas bubble is possible only for the terminal rise velocity of a single air bubble in stagnant liquid. The only quantity which can be varied in this experiment is the bubble diameter, so that the measurements produce a diagram which describes the dependence of the bubble terminal rise velocity on the bubble diameter. It is well known that such experimental results exhibit considerable fluctuations, because the bubble rise velocity depends strongly on the purity of water. Figure 3 shows the curves representing the dependence of the terminal velocity u_{rise} on the diameter of single air bubbles in stagnant tap and distilled water. Both curves are calculated analytically, according to expression 2.11 from Fan and Tsuchiya (1990), where the curve parameters were fitted to the measurement results presented by Haberman and Morton (1953). Note that, particularly in the range of bubble diameters $1 \text{ mm} < d_b < 2 \text{ mm}$, large differences in the rise velocity of single bubbles are observed. These differences are due to the

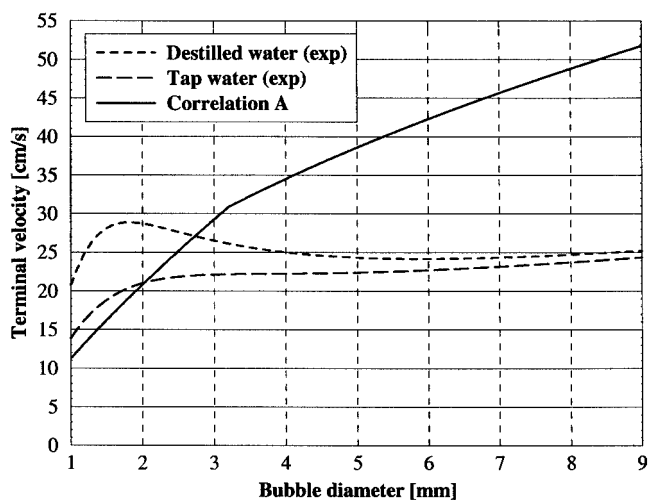


Figure 3. Terminal velocity u_{rise} of single bubbles in stagnant tap and distilled water, according to expression 2.11 from Fan and Tsuchiya (1990).

Solid line-terminal velocity u_{rise} calculated from Eq. 27 for Correlation A (see Table 1).

fact that, as a result of surface-active impurities in tap water, the bubble surface is immobilized, which decreases the bubble rise velocity (Wesselingh, 1987).

Since the experimental information available to date is insufficient to determine unambiguously the drag coefficient C_d as a function of the three dimensionless numbers, the literature abounds with various controversial correlations.

Some frequently used correlations for the drag coefficient C_d are presented in Table 1. A very simple expression for the drag force was proposed by Schwarz and Turner (1988). They lump the product $1/2 C_d \rho_l \pi (d_b^2/4) |\mathbf{u}_b - \mathbf{u}_l|$ to $C_w V_b$, so that the expression 23 for the drag force is simplified to

$$F_d = -C_w V_b (\mathbf{u}_b - \mathbf{u}_l) \quad (24)$$

with a constant value for C_w (Correlation F)

$$C_w = 5 \times 10^4 \frac{\text{kg}}{\text{m}^3 \cdot \text{s}}, \quad (25)$$

leading to a mean bubble slip velocity of about 20 cm/s, which agrees well with experimental values for air bubbles in tap water.

An essential advantage of this approach lies in the fact that this correlation enables a direct calculation of the slip velocity $\mathbf{u}_{\text{slip}} := \mathbf{u}_b - \mathbf{u}_l$ from

$$\mathbf{u}_{\text{slip}} = -\frac{\nabla p}{C_w} \quad (26)$$

if the only forces to be taken into account are the pressure force 20 and the drag force 24, while all other correlations from Table 1 require the computationally expensive iterative procedure for the calculation of the slip velocity.

Due to its simplicity, correlation F was used by many authors (Becker et al., 1994; Deng et al., 1996; Grienberger and

Table 1. Frequently Used Correlations for the Drag Coefficient C_d (Both Expressions for E are Equivalent)

No.	Correlation	Ref.
A	$C_d = \begin{cases} \frac{24}{Re} (1 + 0.15Re^{0.687}), & \text{if } Re < 1,000 \\ 0.44, & \text{if } Re \geq 1,000 \end{cases}$	Delnoij et al. (1997a,b) Djebbar et al. (1996) Kuwagi and Ozoe (1999) Mudde and Simonin (1999) Sommerfeld et al. (1997)
B	$C_d = \text{Max} \left[\frac{24}{Re} (1 + 0.15Re^{0.687}), \frac{8}{3} \cdot \frac{E\ddot{o}}{E\ddot{o} + 4} \right]$	Pan et al. (1999, 2000) Tomiya et al. (1995a) Tomiya (1998) Tsuchiya et al. (1997)
C	$C_d = \frac{0.622}{\frac{1.0}{E\ddot{o}} + 0.235}$	Bhanu and Mazumdar (1997) Jakobsen et al. (1997) Johnansen and Boysan (1988) Ranade and van den Akker (1994)
D	$C_d = \begin{cases} 24/Re, & \text{if } Re < 0.49 \\ 20.68/Re^{0.643}, & \text{if } 0.49 < Re < 100 \\ 6.3/Re^{0.385}, & \text{if } Re > 100, We \leq 8 \text{ and } Re \leq 2,065.1/We^{2.6} \\ We/3, & \text{if } Re > 100, We \leq 8 \text{ and } Re > 2,065.1/We^{2.6} \\ 8/3, & \text{if } Re > 100, We > 8 \end{cases}$	Boisson and Malin (1996) Ilegbusi et al. (1998) Jenne (1999) Kuo and Wallis (1988)
E	$C_d = \frac{2}{3} E\ddot{o}^{1/2}$ <p style="text-align: center;">or</p> $C_d = \frac{2}{3} d_b \sqrt{\frac{8\rho_l}{\sigma}}$	CFD-Software Package CFX 4.2 (AEA Technologies) Ishii and Zuber (1979) Morud (1994) Morud and Hjertager (1996)

Hofmann, 1992; Hillmer et al., 1994; Kuzmin, 1999; Lapin et al., 2001; Sokolichin and Eigenberger, 1994; Svendsen et al., 1992; Torvik and Svendsen, 1990).

Sokolichin and Eigenberger (1999) and Borchers et al. (1999) assumed a constant bubble slip velocity of 20 cm/s and reported a very good agreement with experiment for a series of test cases of steady-state and dynamic turbulent bubbly flows in a locally aerated bubble column with different aspect ratios. We will use one of their examples to discuss the sensitivity of the simulated fluid dynamics on the bubble slip velocity assumed.

A flat bubble column with 2.0 m height, 0.5 m width and 0.08 m depth was considered. The liquid height equals 1.0 m, which corresponds to the aspect ratio H/D of 2. The gas is dispersed by means of a frit sparger centrally located at the bottom of the column. At superficial gas velocity of 0.4125 mm/s, which corresponds to gas throughput of 1 L/min, the flow in the flat bubble column has a quasi-periodic character.

Liquid vortices which move downwards on the lefthand and righthand sides of the column are responsible for the oscillatory motion of the bubble swarm shown on the left of Figure 4. Isolines of the gas volume fraction from the corresponding simulation are displayed in the middle, and vector plots of the liquid velocity can be seen on the righthand side. Experimental and simulated results are in good accord concerning shape, bubble dispersion close to the liquid surface, and time period of oscillations.

A quantitative comparison of LDA measured and calculated liquid velocity data is presented in Figure 5. Since *dynamic* measurements with LDA are restricted to single points, only the *time-averaged* velocity patterns can be compared with respective simulation results. With this long-time averaging, the oscillations caused by moving vortices result in a symmetric flow structure.

The long-time averaged flow map of liquid velocity shows two vortices on both sides of the bubble swarm (Figure 5a). A

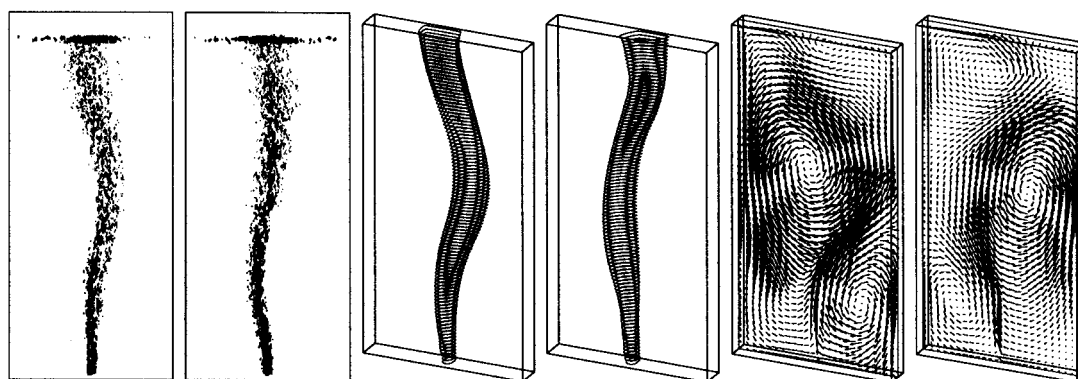


Figure 4. Oscillating flow in the flat bubble column.

Bubble swarm images (left), calculated gas holdup (center), and liquid velocity field (right) at two different times (Borchers et al., 1999).

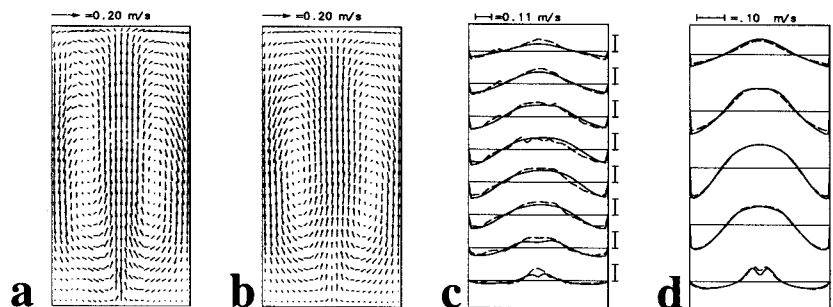


Figure 5. Long-term averaged liquid velocity maps in the mid-depth plane of the bubble column of Figure 4.

LDA measurements (a) and simulations (b), comparison of measured (---) and calculated (—) 1-D liquid velocity profiles (c) from Borchers et al. (1999). Comparison of liquid velocity profiles at different heights calculated with $u_{\text{slip}} = 20$ cm/s (—) and with $u_{\text{slip}} = 25$ cm/s (---) (d).

similar flow structure was obtained in the simulations (Figure 5b). Also, 1-D velocity profiles at different heights (Figure 5c) show good agreement of experiments and simulations. Differences occur only in the region directly above the gas sparger where the flow has a very turbulent, chaotic structure.

In the underlying experiment, gas bubbles with equivalent diameters of 2 to 6 mm were mainly observed. Figure 3 illustrates that for bubbles with diameters above 1.5 mm their terminal velocity in the tap water varies in the range between 20 and 25 cm/s. Our assumption of a constant slip velocity of 20 cm/s corresponds to the lower bound of this range. To investigate the influence of the slip velocity on the simulation results, we performed comparative simulations with the slip velocity set equal to 25 cm/s. The results for both values of the slip velocity are presented in Figure 5d. It is evident that the calculated liquid velocity profiles do not respond very sensitively to the variation of u_{slip} . Similar comparisons were performed for all test cases from Sokolichin and Eigenberger (1999) and Borchers et al. (1999). The weak dependence of the simulation results on the employed value of the slip velocity was observed for all test cases.

This phenomenon is due to the fact that a 25% increase in the slip velocity from 20 cm/s to 25 cm/s does not necessarily lead to an equivalent increase in the vertical bubble velocity. For example, in the flat bubble column with an aspect ratio of 2 presented in Figures 4 and 5, the instantaneous vertical velocity of the liquid phase (which is substantially higher than the long-time averaged velocity depicted in Figure 5c) along the bubble trajectory lies in the range of 30 cm/s, so that an increase in the slip velocity of 25% results in an increase of the vertical bubble velocity (which can be represented as a sum of the liquid velocity and slip velocity) of just 10%.

Nevertheless, the assumption of a constant slip velocity, as well as the application of correlation F for the calculation of the drag force, has often been questioned since the dependence of the slip velocity on the bubble diameter is completely neglected. Therefore, it would be interesting to investigate how well this dependency is reproduced by other correlations presented in Table 1.

For a single bubble rising with a constant velocity in the stagnant water, the rise velocity can be calculated from the equilibrium between the pressure force, gravity, and drag force. If we neglect the gravity (which is much smaller than the pressure force), we obtain

$$u_{\text{rise}} = \sqrt{\frac{4}{3} \cdot \frac{d_b g}{C_d}} \quad (27)$$

The values for the bubble rise velocity calculated from this formula using correlations A to E are represented in Figures 3 and 6. It is seen from Figure 3 that correlation A results in values of the bubble rise velocity, which are considerably overestimated for bubble diameters above 3 mm.

Not all publications which use this correlation specify explicitly the employed value for the bubble diameter, so that in such cases it is unclear, whether or not the resulting relative velocity between both phases lies in the region corresponding to the measurements (for $2 \text{ mm} < d_b < 2.7 \text{ mm}$). Sommerfeld et al. (1997), as well as Mudde and Simonin (1999), simulated the locally aerated bubble column from Becker et al. (1994) using a bubble diameter of $d_b = 3 \text{ mm}$, which agrees with the averaged bubble diameter measured in the underlying experiment, but results (according to correlation A) in an overestimated bubble rise velocity of about 29 cm/s. Delnoij et al. (1997a) resort to a fictitious bubble diameter of 2 mm for the

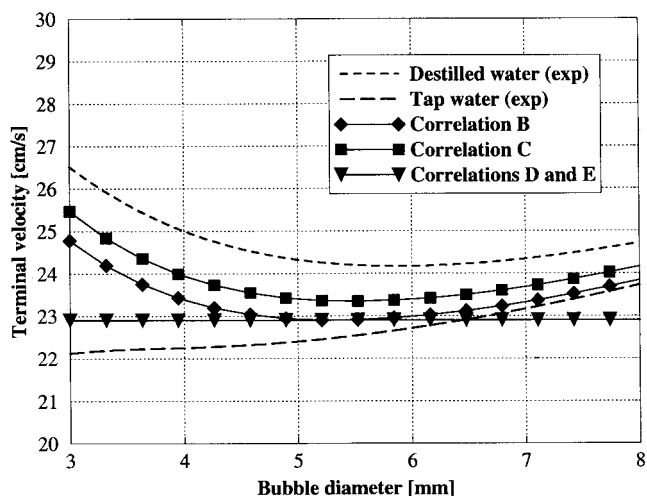


Figure 6. Terminal velocity u_{rise} of single bubbles in stagnant water calculated from Eq. 27 for correlations B to E (see Table 1).

same test case to obtain a more realistic bubble rise velocity of just 20.8 cm/s.

The application of correlations B and C in connection with Eq. 27 results in a dependence of the bubble rise velocity on the bubble diameter which lies in the area between the two experimentally determined curves for the distilled and tap water. However, this dependence is not very strong. In fact, for bubble diameters $4 \text{ mm} < d_b < 7.8 \text{ mm}$, both curves predict terminal rise velocities in a very narrow range between 23 and 24 cm/s (Figure 6).

The result produced by correlation D is very surprising. Although this correlation implies a very detailed representation, it results in a bubble rise velocity which is independent of the bubble size, if the bubble diameter is greater than $d_b = 2.27 \text{ mm}$ and the restriction $We \leq 8$ applies. Insertion of $C_d = We/3$ into Eq. 27 leads to the following expression for the bubble rise velocity

$$u_{\text{rise}} = \sqrt[4]{\frac{4\sigma g}{\rho_l}} \approx 22.9 \frac{\text{cm}}{\text{s}} \quad (28)$$

The use of correlation E produces the same results not only for bubble diameters above $d_b = 2.27 \text{ mm}$, but for all bubble sizes.

In summary we can state that, apart from correlation A, all correlations examined above provide reasonable estimates for the bubble rise velocity. However, the differences between the resulting curves are marginal, and they exhibit little (if any) dependence on the bubble diameter.

Remark. All correlations for the drag coefficient discussed so far were tested only for the case of stagnant liquid, and it remains unclear how well the different correlations approximate the drag force if the relative velocity between both phases deviates from the terminal rise velocity of bubbles. A second important uncertainty factor is introduced by the collective behavior of bubbles in a swarm and its influence on the resistance of individual bubbles. All correlations for the drag coefficient discussed so far refer to the rise of isolated gas bubbles. In a mathematical model, the influence of the bubble swarm is usually taken into account by multiplying the drag correlations derived for a single bubble by a correction factor which depends on the local gas content (Morud and Hjertager, 1996; Tomiyama, 1998; Mudde and Simonin, 1999; Pan et al., 2000). Unfortunately, the question as to whether the resistance of a gas bubble in the swarm is higher or lower than that of a single rising bubble is still largely unresolved (Schlueter and Raebiger, 1998). Recent experimental evidence of Borchers (2002) supports a correlation of Richardson and Zaki (1954), which—in accord with physical intuition—suggests an increase of the resistance with increasing gas holdup.

Added mass force

The drag force takes into account the interaction forces between the liquid and bubbles in a uniform flow field under nonaccelerating conditions. However, if the bubbles accelerate relative to the liquid, part of the surrounding liquid has to be accelerated as well. This additional force contribution is called the “added mass force” and can be calculated from

$$F_{\text{am}} = -C_{\text{am}} V_b \rho_l \frac{Du_{\text{slip}}}{Dt}$$

where the coefficient C_{am} corresponds to the volume fraction of liquid which is accelerated with the bubble. Then, the expression for F_{am} represents nothing else but the mass of the entrained liquid multiplied by the relative acceleration between the two phases. Without the effect of the added mass, a bubble released at the gas sparger would experience a very high acceleration under the influence of Archimedes’ buoyancy. The added mass increases the effective inertia of the gas bubble considerably and delays the adjustment of its terminal rise velocity.

Unfortunately in a system where both phases are accelerated independently, the material derivative Du_{slip}/Dt appears not to be well defined. Most of the two-fluid models presented in the literature use the approximation (see also Jakobsen et al., 1997)

$$\frac{Du_{\text{slip}}}{Dt} = \frac{Du_g}{Dt} - \frac{Du_l}{Dt},$$

where the operator D/Dt denotes the total time derivatives in two phases. If the motion of single gas bubbles in the Lagrangian frame of reference is considered, the total derivative Du_g/Dt should be replaced by the bubble acceleration du_g/dt along its trajectory, leading to

$$F_{\text{am}} = -C_{\text{am}} V_b \rho_l \left(\frac{du_b}{dt} - \frac{Du_l}{Dt} \right) \quad (29)$$

Although the influence of the added mass is generally accepted because of its physical plausibility, it is rather difficult to estimate the value of the parameter C_{am} correctly. While the theoretical investigations have so far been limited to oversimplified models, the experimental determination of this coefficient is complicated by the fact that, in the experiments performed up to now, the influence of the added mass on the measurement results was found to be extremely weak (Hsieh, 1988). The basic difficulty of the experimental determination of the added mass coefficient lies in the fact that the influence of the added mass force can be seen only when high frequency fluctuations in the slip velocity occur (Drew, 1983). In the experiment, it is, however, very difficult to adjust and to analyze such changes reliably enough. These uncertainties explain why many different correlations for the coefficient C_{am} can be found in the literature (see, for example, Jakobsen et al., 1997). The overwhelming majority of authors, who consider the added mass force in the simulations of bubbly flows, use the value of $C_{\text{am}} = 0.5$ (Bhanu and Mazumdar, 1997; Jenne, 1999; Kuwagi and Ozoe, 1999; Lain et al., 1999; Mudde and Simonin, 1999; Pan et al., 1997; Park and Yang, 1997; Smith and Milelli, 1998).

In addition to the many different representations for the added mass coefficient, it is also disputed whether the consideration of the added mass force has any noticeable influence on bubble flow simulation results. The assumption that the added mass force can be safely neglected is based on the premise that the gas bubble reaches its terminal velocity very fast. To show this premise, we consider the ascent of a single gas bubble

being initially at rest in a stagnant water of infinite extent. For the sake of simplicity, we use correlation F (Eqs. 24 and 25) for the drag coefficient. Because of $u_l = 0$ and $\partial p / \partial x = -\rho_l g$, the (1-D) equation of motion for the gas bubble reads in this case

$$\frac{d(m_b u_b)}{dt} = V_b \rho_l g - m_b g - C_w V_b u_b - C_{am} V_b \rho_l \frac{du_b}{dt} \quad (30)$$

or

$$\left(1 + \frac{\rho_l}{\rho_g} C_{am}\right) \frac{du_b}{dt} = -\frac{C_w}{\rho_g} u_b + \left(\frac{\rho_l}{\rho_g} - 1\right) g \quad (31)$$

Because of $(\rho_l / \rho_g) \gg 1$, it is obvious that the inertia and gravity force terms can be neglected in comparison with the added mass and the pressure force

$$C_{am} \rho_l \frac{du_b}{dt} = -C_w u_b + \rho_l g \quad (32)$$

The analytical solution of this equation with the initial condition $u_b(0) = 0$ is

$$u_b(t) = \frac{\rho_l g}{C_w} (1 - e^{-C_w t / (C_{am} \rho_l)}) \quad (33)$$

or, using $\rho_l = 1,000 \text{ kg/m}^3$, $g \approx 10 \text{ m/s}^2$, $C_w = 5 \times 10^4 \text{ kg/m}^3 \cdot \text{s}$ and $C_{am} = 0.5$

$$u_b(t) = 0.2 \frac{\text{m}}{\text{s}} (1 - e^{-100t}) \quad (34)$$

This means that the terminal rise velocity is already achieved after less than one-tenth of a second. Since the relaxation time of a gas bubble is as small as 0.01 s, added mass force would only be visible if the velocity of the liquid phase along the bubble trajectory exhibits high frequency oscillations. This conclusion agrees with that of Drew (1983). One could think here of the influence from turbulent fluctuations, in particular, in the bubble swarm. However, these fluctuations are not resolved in the framework of a two fluid model, since it contains only averaged quantities.

The above conclusions are also supported by Jenne (1999) who investigated the influence of the added mass force on the distribution of the gas phase in a stirred tank reactor. Although, in a mechanically agitated gas-liquid tank at a high rotation frequency of impeller(s), the velocity field is subject to substantially higher fluctuations as in the case of bubbly-driven flows, no qualitative and, hardly any quantitative, differences between the simulations with and without the consideration of the added mass force were observed (see Figure 60 in Jenne (1999)).

Life force

If a **rigid spherical particle** moves in a nonuniform flow field, additional forces perpendicular to the main flow direction

occur. These forces result from the asymmetric pressure distribution around the particle. The Saffman force is due to the shear in the mean flow and is experienced by the solid particle even if it doesn't rotate. The Magnus force, on the other hand, results from the asymmetric pressure distribution which follows from a particle rotation even if the flow field is uniform and has no shear (far away from the particle).

There are many different representations for the sum of these forces which is often called the "transversal lift force." Since, for bubble flow, the transversal lift force has been used to influence the radial redistribution of the gas bubbles in a vertically aligned flow field, the notions "radial" or "lateral lift force" are also common. As in the case of the drag force, the lift force can be calculated theoretically only in the simplest cases. For the determination of the Saffman force, rigid spherical particles at low Reynolds numbers are considered, and the Magnus force is calculated under the assumption of ideal inviscid flow conditions. However, in bubbly flows the phenomenon is much more complex (formulation of an asymmetric wake, bubble deformation, and flow inside the bubble) and admits no accurate theoretical description. A straightforward transfer of the expressions derived under the idealized assumptions for the simulation of real bubbly flows is, therefore, not justified.

On the one hand, for the range of Eötvös-, Morton-, and Reynolds numbers relevant for the bubble flow, there currently exists no unambiguous experimental evidence or theoretical proof for the existence, the direction, and the magnitude of the radial force. On the other hand, most formulations of the radial force have a *very strong* influence on the simulation results. Therefore, the radial force can be abused for achieving an improvement of simulation results through a nonphysical adjustment of parameters contained in the radial force representation.

We would like to illustrate this with some examples. Let us consider the representation for the lift force, which was deduced by Auton (1987), as well as Thomas et al. (1983), for the case of a potential flow around a spherical particle and which is used in most articles on the simulation of bubbly flows which consider the lift force

$$\mathbf{F}_l = -C_l V_b \rho_l (\mathbf{u}_b - \mathbf{u}_l) \times (\nabla \times \mathbf{u}_l) \quad (35)$$

The references cited adopt a value $C_l = 0.5$ for the lift coefficient, which has also been used by Delnoij et al., 1997a,b, 1999; Kuwagi and Ozoe, 1999; Murai and Matsumoto, 1998; Smith and Milelli, 1998. Other authors however use much smaller positive values (such as $C_l = 0.01$ in Lahey (1990)), as well as negative (!) values between -0.5 and -3.0 , in order to obtain agreement between simulation and experiment.

The effect of the lift force on the bubble trajectory can be most simply illustrated if we assume an axisymmetric developed flow in the central region of a vertical cylinder. In this case only the axial component of the liquid velocity (u_l^x) differs from zero and can vary only in the radial direction. Therefore, we can calculate the radial component of the lift force from

$$F_l^r = -C_l V_b \rho_l (u_b^x - u_l^x) \frac{\partial u_l^x}{\partial r}. \quad (36)$$

Here u_b^x and u_l^x stand for the axial velocity of the bubble and of the liquid phase. Furthermore, if the axial velocity of the liquid phase decreases towards the wall, we have

$$\frac{\partial u_l^x}{\partial r} < 0 \quad (37)$$

Since the inequality

$$u_b^x - u_l^x = u_{\text{slip}}^x > 0 \quad (38)$$

is valid, we can conclude from Eq. 36 that the direction of the radial force is related to the sign of C_l : for $C_l > 0$ it acts towards the wall, while, in the case $C_l < 0$, it drives the bubbles to the center of the cylinder. Therefore, either positive or negative values for the lift coefficient have been used, depending on whether the redistribution of the radial gas holdup profile towards the wall or towards the cylinder center was needed for a better agreement between the simulation results and experimental data.

In the case of an enforced upward flow in a vertically aligned **pipe** some experimental data show that the gas holdup profiles exhibit a pronounced maximum near the wall in the developed flow region, even if the gas is fed into the pipe uniformly over the entire cross section (Liu, 1989; Serizawa et al., 1986; Wang et al., 1987). To achieve a good agreement with the measurement data, one needs to reshape the initially flat gas holdup profile by means of a lift force, which shifts the gas bubbles towards the wall. Accordingly, a **positive** value for the lift coefficient is used in this case.

The corresponding experiments are usually performed in long pipes with diameters of just a few centimeters, and the liquid velocity in the center of the pipe typically lies in the range of 1–2 m/s. In this case the application of the theoretically deduced value for the lift coefficient ($C_l = 0.5$) would lead to a radial force corresponding to a *horizontal* slip velocity of 10–20 cm/s. Therefore a substantially lower value of C_l is used for the simulation of bubbly flow in a pipe. For instance, Lopez de Bertodano et al. (1994b) suggest values between 0.02 and 0.1.

In contrast, in the case of a **uniformly aerated bubble column**, the gas holdup profiles exhibit a maximum not in the wall region, but in the center of the reactor (Grienberger, 1992; Hills, 1974). This means that the gas holdup profile (which is flat directly above the gas sparger) shifts towards the central axis of the bubble column. Since a positive value of the lift force coefficient would lead to exactly the opposite trend, the **sign** of the coefficient has been **reversed**, to achieve a better agreement with the measured gas holdup profiles.

Because the change of the axial velocity in the radial direction in a bubble column is about one order of magnitude smaller than in the vertical pipe flow discussed above, the *absolute* value of the lift coefficient used in the simulations of bubble columns has to be essentially higher than in the case of the pipe flow and was set to -0.5 by Boisson and Malin (1996), Grienberger and Hofmann (1992), and Torvik and Svendsen (1990), to -1.5 and -2.0 by Jakobsen et al. (1997), and even to -3.0 by Svendsen et al. (1992). These values of the lift coefficient would correspond to a horizontal slip velocity approximately 2 to 6 cm/s directed to the center of the column. The strong influence of the value employed

becomes evident from Figure 5.8 from Grienberger (1992): while the liquid velocity in the center of the column calculated with a value $C_l = -0.1$ equals to 16 cm/s, the lift coefficient $C_l = -0.7$ results in an almost four times higher axial velocity of 60 cm/s.

Results of some experimental investigations as well as results of the direct numerical simulation of a single bubble rising in a shear flow reveal that a transversal force acting on the bubble can develop and that the direction of this force depends on the *bubble size* (Esmaeeli et al., 1994; Tomiyama et al., 1995b). Therefore, Tomiyama et al. (1995b) propose the following formulation for the lift coefficient, which depends on the bubble diameter

$$C_l = -0.04E\delta + 0.48 \quad (39)$$

For air bubbles in water, this corresponds to a negative sign for bubble diameters greater than 9 mm; the value $C_l = -0.5$ corresponds to a bubble diameter of approximately 13 mm. It should be noted, however, that the direct numerical simulations, as well as the experiments, were performed for the Morton numbers which lie in the range of $-5 < \log(Mo) < -3$. Therefore, they apply to fluids, which have a substantially higher viscosity than water. The sign change of the lift coefficient is justified by the fact that, for large bubbles, the wake develops symmetrically due to bubble deformation, so that the interaction between the shear flow and the wake shifted to the wall results in an additional transverse force; this acts in the direction opposite to the “classical” lift force. However, it is very unlikely that this argumentation retains its validity also for large air bubbles in water, since, for air bubbles with diameters above 9 mm, no stable, laterally shifted bubble wake exists. Many experimental results show that even bubbles with substantially smaller diameters are characterized by an *unstable*, dynamic, periodically separating wake (see, for example Fan and Tsuchiya, 1990).

The examples given above reveal a great deal of arbitrariness for the incorporation of the radial force into bubbly flow simulations. This practice has been further compromised by the fact that the lift force was applied mainly in such cases, where it leads to a better agreement with the measurements. This has been the case for buoyancy driven bubble flow in a uniformly aerated bubble column, simulated with steady-state balance equations. However, the need to assume a lateral lift force disappears if the model equations are solved dynamically. The unsteady vertical flow structure then leads to a long-time averaged flow with a higher gas holdup in the column center, resulting in the well-known upflow in the center and downflow at the walls (Devanathan et al., 1995; Sokolichin et al., 1997).

On the relevance of different forces

A particular force should be regarded as a *relevant force* for the mathematical model, only if the following two conditions are satisfied: (1) the existence of this force is experimentally verified; (2) the consideration of this force in the mathematical model has an important influence on the simulation results.

If a given force fulfills both conditions, it should be further investigated whether a reliable model for its numerical computation is available.

The inertia force $[d(m_b u_b)]/dt$, the gravity F_g , and the added mass force F_{am} , whose existence is undisputed, have

shown to exert virtually no influence on the simulation results. Since the consideration of these forces in the mathematical model does not modify the simulation results, the additional computational effort can be saved.

The lift force F_l belongs to the class of nonrelevant forces of the second type: its consideration in the mathematical model has a very strong influence on the simulation results, whereas its existence and sign are still not validated for realistic bubble sizes.

The only two relevant forces according to the definition given above are the pressure force and the drag force. Without the action of the pressure force, a bubble released in stagnant water would not rise, while, without the effect of the drag force, the released bubble would accelerate infinitely.

In summary we can state that those mathematical models, which are limited to the consideration of the pressure force and the drag force, involve all forces previously found to be undisputed and essential.

With this conclusion, we can come back to the momentum balance of the gas bubble. If only the pressure force and the drag force are considered in Eq. 19, then the slip velocity \mathbf{u}_{slip} between the bubble and the liquid phase can be calculated directly from the relationship $0 = \mathbf{F}_p + \mathbf{F}_d$

$$\frac{3}{4} \frac{C_d}{d_b} \rho_l |\mathbf{u}_{\text{slip}}| \mathbf{u}_{\text{slip}} = -\nabla p \quad (40)$$

from which the bubble velocity \mathbf{u}_l can be determined as

$$\mathbf{u}_b = \mathbf{u}_l + \mathbf{u}_{\text{slip}} \quad (41)$$

Modeling of the bubble path dispersion

If we take a look at a snapshot of a bubbly flow in a locally aerated bubble column (see, for example, Figure 4, left), we see that the width of the rising bubble swarm increases with the height of the column. Thus, a radial mixing takes place in the gas phase. An axial mixing in the gas phase also takes place, but its effect cannot be recognized because the convective transport dominates in the vertical direction.

The bubble path diffusion results from the interactions between the bubbles on the one hand, and from the influence of the liquid phase turbulence on the other hand. The relative motion of the bubbles in the liquid leads to strong fluctuations of the liquid velocity in the direct neighborhood of individual gas bubbles and particularly inside the bubble wake. These fluctuations affect the behavior of the neighboring bubbles. Smaller bubbles can be accelerated in the wake of the large bubbles, and others are pushed aside. If the flow has a global turbulent character, then the diffusive effects, which result from the bubble interactions, are *additionally* enhanced by the turbulent eddies in the liquid phase. For relatively low gas holdups and small bubble sizes, this turbulent mixing effect is often even more pronounced than the diffusion caused by bubble interaction.

The question arises concerning where the bubble dispersion has to be considered in the model equations. The only plausible answer is: in the gas phase continuity Eq. 18. One has to realize that so far we have only talked about the (individual) bubble rise velocity \mathbf{u}_b . Compared to \mathbf{u}_b , the gas phase velocity \mathbf{u}_g is a *phase-averaged* quantity which may contain an additional

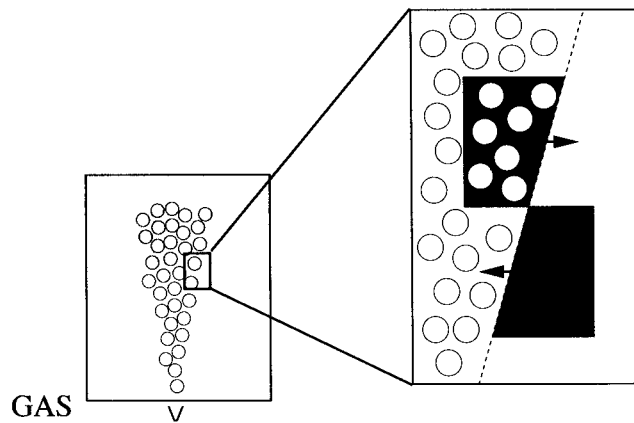


Figure 7. Dispersion of a locally aerated bubble plume (left), caused by the turbulent exchange of equal size gas/liquid volume elements.

component $\mathbf{u}_{\text{drift}}$. This contribution called the “drifting velocity” by Simonin and Violet (1990) depends on the local gradient of the volume fraction of the gas phase.

To explain this, we consider the rise of a bubble plume (Figure 7). Focusing at the magnified volume element on the righthand side border of the plume, we look at the bubble movement due to turbulent lateral fluctuations of gas/liquid volume elements. Due to continuity, each volume element moving to the right has to be compensated by a volume element of equal size moving to the left, so that the net volume flux is zero. However, since the gas or liquid fractions of the exchange elements are different, the turbulent exchange results in a net flux of gas from left to right and a corresponding net flux of liquid from right to left.

The exchange flux can be transformed into the above mentioned drifting velocity, which, according to Simonin and Violet (1990), can be calculated from

$$\mathbf{u}_{\text{drift}} = -\mathbf{D}_{gl}^{\text{turb}} \cdot \frac{1}{\varepsilon_g} \nabla \varepsilon_g \quad (42)$$

$\mathbf{D}_{gl}^{\text{turb}}$ stands for the turbulent diffusion tensor. It is usually assumed that this tensor has a diagonal form, whereby all diagonal elements are equal and can be calculated as

$$(\mathbf{D}_{gl}^{\text{turb}})_{ii} = \frac{1}{Sc} \cdot \frac{\mu_l^{\text{turb}}}{\rho_l} \quad (43)$$

Here, μ_l^{turb} denotes the turbulent viscosity of the continuous phase. Sc is the Schmidt number for the turbulent transport and corresponds to the ratio of the velocity fluctuations of both phases. It is experimentally proven that, in the case of gas-liquid flows, the velocity fluctuations of both phases have the same order of magnitude because the light gas bubbles follow the liquid fluctuations immediately (Serizawa, 1974). Therefore, the value $Sc = 1$ is usually taken for the turbulent Schmidt number (Jenne, 1999; Torvik and Svendsen, 1990).

The phase-averaged gas velocity is now the sum of the bubble velocity plus the drift velocity

$$\mathbf{u}_g = \mathbf{u}_b - \frac{\mu_l^{\text{turb}}}{\rho_l} \frac{1}{\varepsilon_g} \nabla \varepsilon_g. \quad (44)$$

If we insert it into the continuity equation for the gas phase (Eq. 18), we obtain the following convection-diffusion equation, which describes both the convective transport and the turbulent mixing in the gas phase

$$\frac{\partial(\varepsilon_g \rho_g)}{\partial t} + \nabla \cdot (\varepsilon_g \rho_g \mathbf{u}_b) = \frac{\partial}{\partial x_i} \left(\frac{\rho_g}{\rho_l} \cdot \mu_l^{\text{turb}} \cdot \frac{\partial \varepsilon_g}{\partial x_i} \right) \quad (45)$$

If the full continuity Eq. 6 of the liquid phase would be used, a similar turbulent mixing term had to be added in order to retain global continuity. However, since we already neglected variations of ε_l (Eq. 7), no further adjustment is necessary.

Modeling of Turbulence

The modeling of turbulence in the continuous phase (the term $\mathbf{T}_l^{\text{turb}}$ in Eq. 14) is one of the main unresolved problems within the two-fluid approach. In the majority of publications on numerical simulations of turbulent bubbly flows, the standard k - ε model developed for single-phase flows has been employed.

k - ε turbulence model

The standard k - ε turbulence model makes use of the Boussinesq hypothesis (Boussinesq, 1877), according to which the following representation for the turbulent stress tensor $\mathbf{T}_l^{\text{turb}}$ can be applied

$$(\mathbf{T}_l^{\text{turb}})_{ij} = \mu_l^{\text{turb}} \left(\frac{\partial(\mathbf{u}_l)_i}{\partial x_j} + \frac{\partial(\mathbf{u}_l)_j}{\partial x_i} \right) - \frac{2}{3} \rho_l \delta_{ij} k \quad (46)$$

The turbulent eddy viscosity μ_l^{turb} is calculated from

$$\mu_l^{\text{turb}} = 0.09 \cdot \rho_l \frac{k^2}{\varepsilon} \quad (47)$$

where k is the turbulent kinetic energy, and ε is its dissipation rate, calculated from the well known k and ε equations as specified, for example, in Ferziger and Peric (1996). The general applicability of this model to nonstationary two-phase flows is, however, disputed.

In some contributions no turbulence model is used at all and the influence of this term in the momentum balance equation is simply neglected. The main argument in these cases is that the standard turbulence models, developed for steady-state single-phase flow, will overestimate the value of the effective viscosity and, therefore, completely dampen the transient character of the flow rather than suppress merely the small-scale turbulent fluctuations. As shown by Sokolichin and Eigenberger (1999), this argument seemed to be true if a 2-D k - ε turbulence model was used to simulate the dynamics of a locally aerated flat bubble column similar to that presented in Figure 4. In this case a grid independent solution could be computed on a relatively coarse grid, but the dynamic nature of the flow was completely suppressed by the strong turbulent viscosity. Neglecting turbu-

lent viscosity led to a dynamic solution in close agreement with the experiments, but this solution was not grid-independent. Only after a full 3-D turbulent model was used did the simulation results show a good agreement with experiments. The explanation was that in a *flat* bubble column turbulence is reduced substantially if the true depth of the column is considered as compared to the 2-D case with unlimited column depth.

Borchers et al. (1999) used the 3-D-standard k - ε model for a series of test cases of steady-state and dynamic turbulent bubbly flows in a locally aerated bubble column with different aspect ratios. In all test cases a very good agreement with experiments was achieved. It is, however, obvious that the general applicability of the 3-D k - ε -turbulence model to the dynamic simulation of bubbly flows is questionable since it completely neglects the turbulence induced by the gas phase.

Bubble induced turbulence

In the test cases of locally aerated flat bubble columns mentioned above, the gas phase occupied only a small part of the reactor. This may be the reason why the influence of the bubble-induced turbulence could be neglected. Figure 8 presents a test case of a flat airlift loop reactor with 2.0 m height, 0.5 m width, and 0.08 m depth. A central inner wall (1.45 m height, 0.03 m width located 16 cm above the bottom) separates the two main parts of the bubble column. The liquid height equals 1.9 m. The gas is dispersed by a frit sparger located 15 cm from the lefthand side of the reactor, the gas-flow rate equals 4 L/min. A photo of the more or less steady bubble distribution and the LDA-measurements of the circulating liquid velocities in the mid-depth plane are presented on the lefthand side of Figure 8. The corresponding (grid independent) simulation results, obtained with the 3-D, dynamic model (Eqs. 13–15, 17, 41, 45, 46, 47) under the assumption of a constant slip velocity of 20 cm/s and application of a standard k - ε model are shown in the center of the figure.

Although the measured and the calculated velocity fields look quite similar, there are some important differences between the experimental results and the simulation. It can be seen that the diffusion in the gas phase is strongly underestimated, so that the gas bubbles accumulate exclusively near the left reactor wall, while a more uniform distribution is observed in the experiment. As a result of this discrepancy, the vertical velocities of the liquid phase are strongly overestimated in the upper part of the riser. A comparison between the measured and the calculated profiles of the turbulent kinetic energy also reveals substantial differences. In this case the gas phase occupies a major part of the riser cross-section, so that the bubble-induced turbulence could be of the same order of magnitude as the shear-induced one. The neglect of this effect in the model obviously leads to an underestimation of the turbulence intensity in the simulation.

The development of mathematical models for the bubble-induced turbulence is still at its infancy. In principle, the conservation equations for the turbulent kinetic energy and its dissipation rate in a two-phase flow can be derived in analogy to the single-phase case (Elghobashi and Abou-Arab, 1983; Kataoka and Serizawa, 1989). However, the lack of sufficient knowledge of the physical processes makes the postulation of closure relations very difficult. As the investigations of gas-solid flows showed, the presence of solid particles can lead

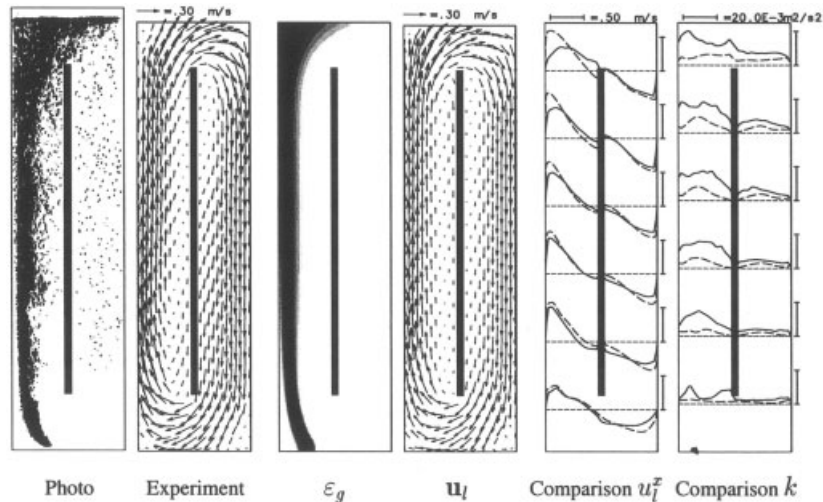


Figure 8. Flat column airlift loop reactor, 4 L/min gas flow.

Experiments and simulation results obtained with standard k - ε model without consideration of the bubble-induced turbulence. From left to right: image of the bubble swarm, LDA-measurements of the flow map in the mid-depth plane, calculated gas holdup and flow map in the mid-depth plane, comparison of measured (—) and calculated (---) liquid velocity, and turbulent kinetic energy profiles at different heights.

either to a reduction or to an increase of the turbulent kinetic energy in the continuous phase, depending on the specific flow conditions. In gas-liquid flows, the interaction of the turbulent eddies with the mobile bubble surface constitutes another important mechanism whose experimental studies have been very scarce (Banerjee, 1990). The large bubbles are comparable in size with the energy-carrying eddies, while their dispersive behavior has not yet been sufficiently investigated. Therefore, many of the models available in the literature are contradictory and the model parameters are mostly fitted to the particular problem under consideration.

In the following some of the most popular models for the bubble-induced turbulence will be presented and their influence on the solution of the test case from Figure 8 will be discussed.

The simplest model for the consideration of the bubble influence on the liquid turbulence is due to Sato and Sekoguchi (1975), as well as to Sato et al. (1981). The stress tensor T_l^{turb} is modeled by Eq. 46, where the effective viscosity is split into a shear induced term $\mu_{l,SI}^{\text{turb}}$ and a bubble induced term $\mu_{l,BI}^{\text{turb}}$

$$\mu_l^{\text{turb}} = \mu_{l,SI}^{\text{turb}} + \mu_{l,BI}^{\text{turb}} \quad (48)$$

$\mu_{l,SI}^{\text{turb}}$ is calculated according to Eq. 47 from the quantities k and ε . The bubble-induced viscosity is assumed to be proportional to the local gas holdup and the slip velocity

$$\mu_{l,BI}^{\text{turb}} = 1.2 \frac{D_b}{2} \varepsilon_g \rho_l |\mathbf{u}_{\text{slip}}| \quad (49)$$

In order to estimate the amount of the so defined bubble-induced viscosity, we insert the sample values $D_b = 5$ mm, $\rho_l = 1,000$ kg/m³ and $|\mathbf{u}_{\text{slip}}| = 20$ cm/s into the expression 49, leading to

$$\mu_{l,BI}^{\text{turb}} = 0.6 \cdot \varepsilon_g \left[\frac{\text{kg}}{\text{m} \cdot \text{s}} \right]$$

For a gas holdup of about 5% (this corresponds to the maximum value of gas volume fraction in the lower part of the riser), the bubble-induced viscosity equals

$$\mu_{l,BI}^{\text{turb}} = 0.03 \left[\frac{\text{kg}}{\text{m} \cdot \text{s}} \right].$$

For the test case examined here, this bubble-induced viscosity is almost two orders of magnitude smaller than the shear-induced part of the effective viscosity. Therefore, it can hardly have any influence on the simulation results. Jenne (1999) examined the influence of Sato's model on the simulation of an aerated stirred tank reactor and reported differences of as much as three orders of magnitude between the bubble-induced and the shear-induced parts of the turbulent viscosity, although, in his test case, the values of the gas holdup exceed the 10% level in some parts of the apparatus.

Another approach to the modeling of bubble-induced turbulence is due to Arnold et al. (1988). It is based on the assumption that the influence of the gas bubbles on the liquid turbulence results primarily from the velocity fluctuations, which originate from the displacement of liquid by the rising bubbles. Since, for continuity reasons, such a displacement takes place in the surrounding fluid even if the bubbles rise in a stagnant medium, these fluctuations cannot be interpreted as turbulence in the conventional sense. Therefore, the notion "pseudo-turbulence" is used instead. A theoretical estimate of the influence of these fluctuations can be derived under the assumption of a potential flow around a group of spheres.

If one further assumes a linear superposition of the shear-induced single-phase turbulence and the bubble-induced

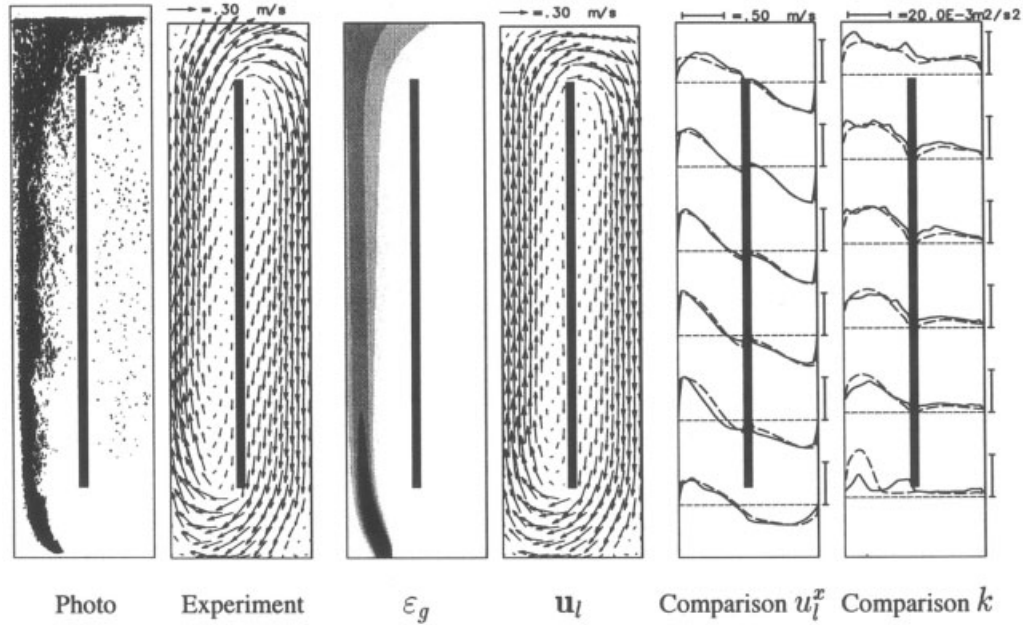


Figure 9. Same as Figure 8, however, simulated with additional source terms (Eqs. 54 and 55) for consideration of the bubble-induced turbulence $C_k = 0.83$, $C_\varepsilon = 0.13$.

pseudo-turbulence, then the stress tensor $\mathbf{T}_l^{\text{turb}}$ can be expressed as

$$\mathbf{T}_l^{\text{turb}} = \mathbf{T}_{l,SI}^{\text{turb}} + \mathbf{T}_{l,BI}^{\text{turb}} \quad (50)$$

where the shear-induced part of the stress tensor is modeled according to Eq. 46 and the bubble-induced pseudo-turbulence is represented through

$$\mathbf{T}_{l,BI}^{\text{turb}} = -\varepsilon_g \rho_l \left[\frac{1}{20} \mathbf{u}_{\text{slip}} \mathbf{u}_{\text{slip}} + \frac{3}{20} \left| \mathbf{u}_{\text{slip}} \right|^2 \mathbf{I} \right] \quad (51)$$

\mathbf{I} denotes here the identity tensor. Lopez de Bertodano et al. (1994a) applied this model in combination with Sato's approach to the simulation of a bubbly flow in a vertical pipe and obtained a remarkable improvement, as compared to simulations performed with the single-phase turbulence model.

For our test case, however, the amount of bubble-induced turbulence calculated with Arnold's model is considerably underestimated. Equation 51 implies that the bubble-induced turbulent kinetic energy can be expressed as follows (Lopez de Bertodano et al., 1994a)

$$k_{BI} = \frac{1}{4} \varepsilon_g \left| \mathbf{u}_{\text{slip}} \right|^2. \quad (52)$$

For the slip velocity of approximately 20 cm/s, this corresponds to

$$k_{BI} = 0.01 \varepsilon_g \left[\frac{\text{m}^2}{\text{s}^2} \right] \quad (53)$$

For $\varepsilon_g \approx 5\%$, this is a factor 20 smaller than the bubble-induced turbulent kinetic energy of $0.01 \text{ m}^2/\text{s}^2$, needed for a reasonable agreement between measured and simulated kinetic energy for the example of Figure 8.

We have seen that both Sato's model and Arnold's model strongly underestimate the bubble-induced turbulence in a number of test cases. Another disadvantage of these approaches consists in their local effect, because they consider the increase of the turbulence intensity only in parts of the reactor where the gas phase is actually present. In reality, the turbulence induced by the bubbles at some given point can spread and affect regions further away from the turbulence source.

The third approach to be discussed for the modeling of bubble-induced turbulence allows for the convective and diffusive transport of turbulent kinetic energy. This model incorporates the influence of the gas bubbles on the turbulence by means of additional source terms in the balance equations for k and ε .

The additional source term in the k -equation is taken to be proportional to the product of the drag force and the slip velocity between the two phases, as proposed by Kataoka and Serizawa (1989). Under the assumption of an equilibrium between the pressure force and the drag force, this term can be represented as follows

$$S_k = -C_k \varepsilon_g \nabla p \cdot \mathbf{u}_{\text{slip}} \quad (54)$$

Since the slip velocity and the pressure gradient are oppositely directed, this term is always positive if the model constant C_k is greater than zero.

The corresponding source term in the ε -equation is usually modeled as

$$S_\varepsilon = C_\varepsilon \cdot \frac{\varepsilon}{k} S_k \quad (55)$$

and is also positive. This means that the contribution of the bubbles both to the production and to the dissipation of the turbulent kinetic energy is positive. The superposition of both effects can result in an increase, as well as in a decrease, of the turbulence intensity compared with the single-phase turbulence model.

In many test cases it is possible to obtain a very good agreement between the experimental data and simulation results by fitting the values of the model constants C_k and C_ε . A better prediction of the measured turbulence intensity is usually accompanied by a better agreement between the measured and calculated liquid velocities.

Also, in our test case the application of this model with (adapted) values of $C_k = 0.83$ and $C_\varepsilon = 0.13$ results in a much better agreement with the experimental data for the profiles of the turbulent kinetic energy, compared to the simulations without bubble-induced turbulence (compare Figure 9 and Figure 8). The higher values of the turbulence intensity lead to a rise in the turbulent diffusion of the gas phase, causing a better agreement between the calculated and the observed gas holdup distribution. The accumulation of the gas content in the center of the riser entails a shift of the velocity peaks in the same direction, so that the correspondence between the measured and computed velocity profiles also improves substantially.

This example demonstrates the importance of a good prediction of the bubble-induced turbulence. Unfortunately, the "optimal" parameter values, determined by fitting of experimental results, differ strongly for each particular case. If the gas flow in the example of Figure 9 is reduced from 4 L/min to 3 and 2 L/min, the optimal values for C_k and C_ε change as shown in Table 2. In all cases a good agreement has been obtained between measurements and simulations (Figure 10), but a clear tendency for the relation of the C_k , C_ε -values from the flow characteristics is not obvious. This agrees with the

Table 2. Optimal Bubble Induced Turbulence Parameters C_k , C_ε of Eqs. 54 and 55 for the Loop Reactor Example with Different Gas Flow

Gas Flow	C_k	C_ε
2 L/min	1.00	1.20
3 L/min	0.84	0.36
4 L/min	0.83	0.13

published literature where the model constants vary between 0.01 and 1 for C_k (Boisson and Malin, 1996; Kuo et al., 1997) and between 1 and 1.92 for C_ε (Bhanu and Mazumdar, 1997; Kuo et al., 1997).

Uniformly Aerated Bubble Columns

The appropriate modeling and simulation of uniformly aerated ("empty") bubble columns still presents the biggest challenge for bubble flow modeling. In the locally aerated bubble columns discussed so far, gas was only present in a part of the column and the local gas volume fraction seldom exceeded 2%. This is in contrast to uniformly aerated bubble columns which often are operated at substantially higher gas content, while the bubbles are spread over the whole column cross section.

A particular challenge is the modeling of bubble columns in the industrially important heterogeneous or churn turbulent regime, which results for high gas throughput (Deckwer, 1992). Small gas bubbles then tend to coalesce to large bubbles which accumulate in the middle of the column and create a strongly turbulent, dynamic flow structure with large 3-D vortices of toroidal shape (Chen et al., 1994). Since these vortices form and move rather randomly, the flow has a strongly chaotic character. So far, mostly long-time averaged flow profiles, but no detailed information about the vortical dynamics, is experimentally available.

The long-time averaged liquid flow velocities in empty and (more or less) uniformly aerated bubble columns result in a so-called gulf stream flow structure similar to Figure 5, where liquid moves upstream in the column center and

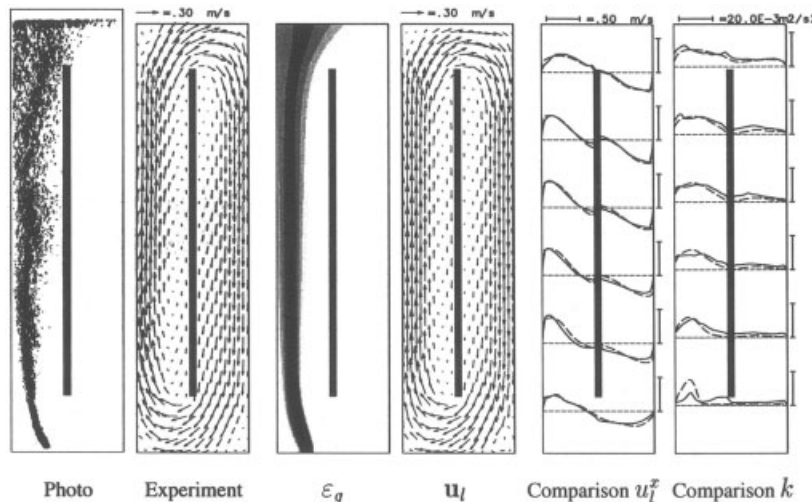


Figure 10. Flat column airlift loop reactor with 2 L/min.

Comparison between experiment and simulation with bubble-induced turbulence $C_k = 1.00$, $C_\varepsilon = 1.2$, from left to right: bubble image, center plane flow map, gas holdup, center plane flow map, axial velocity (u_l^T) profiles and turbulent kinetic (k) energy profiles at different heights (--- simulated, — measured).

Table 3. Definition of 4 Test Cases and The Maximum Value of the Long-Time Averaged Liquid Velocity in the Center of Empty Bubble Column

Case	Turbulence Model	Turbulent Dispersion	Bubble Induced Turbulence	C_k	C_ε	U_{\max}
a	$k-\varepsilon$	No	No	—	—	17.2 cm/s
b	$k-\varepsilon$	Yes	No	—	—	4.2 cm/s
c	$k-\varepsilon$	Yes	Yes	1.0	1.2	0.002 cm/s
d	$k-\varepsilon$	Yes	Yes	1.0	1.92	12.3 cm/s

downstream at the walls (Hills, 1974; Devanathan et al., 1995; Mudde et al., 1997). However, in these long-time averaged results all the strong vortical fluctuations, where local velocities may temporarily exceed the long-time averaged velocities manifold, are leveled out. This means that information about the true local medium to large-scale mixing behavior which may be essential for an appropriate reactor simulation (see Bauer and Eigenberger, 2001) is no longer available.

During the past few years, many contributions concerning the detailed hydrodynamic modeling of empty bubble columns have been published. Whereas earlier work (see Jakobsen et al., 1997 for reference) tried to use 2-D steady-state models with cylindrical coordinates, it has meanwhile been generally accepted that a 3-D unsteady-state model is required to capture the important flow and mixing characteristics. We would like to refer in particular to the work of Pflieger and Becker (2001), who used a 3-D dynamic simulation with a $k-\varepsilon$ turbulence model and bubble induced turbulence to model empty bubble columns.

In their results they considered empty tube gas velocities between 0.15 and 2 cm/s. The bubble column was uniformly aerated over the inner 80% of the bottom surface. Bubble induced turbulence (BIT) was modeled using Eqs. 54 and 55 with $C_k = 1.0$ and $C_\varepsilon = 1.92$. In all cases the simulations

predicted a strongly instationary vortical flow behavior. The long-time averaged velocities agreed well with the measurements. It has to be noted, however, that the authors neglected turbulent dispersion in the gas phase completely.

To study the influence of turbulent dispersion together with the influence of the BIT-parameters on their results, we performed a number of simulations, the details of which are specified in Table 3. In all cases an empty tube gas velocity of 1.6 cm/s was assumed. The dimensions of the cylindrical bubble column studied were 90 cm in height and 15 cm in diameter and the aerator was assumed to cover 80% of the bottom surface. A rectangular grid with $180 \times 30 \times 30$ points mapping the circular cross section was used.

Case a is a simulation with the turbulent $k-\varepsilon$ -model without bubble induced turbulence. As in Pflieger and Becker (2001), no turbulent gas dispersion was considered. Strongly instationary hydrodynamics resulted (Figure 11a) with a large upward liquid flow in the column center as a result of the gas accumulating predominantly near the column axis. This is clearly visible in the snapshot profiles of gas holdup in Figure 12a.

If the influence of turbulence is not only considered in the effective viscosity but also in the turbulent gas dispersion, the dynamic flow character gets almost lost (Figure 11b). The liquid velocity fluctuations over the sparger now die out quickly. This is a consequence of the strong turbulent gas

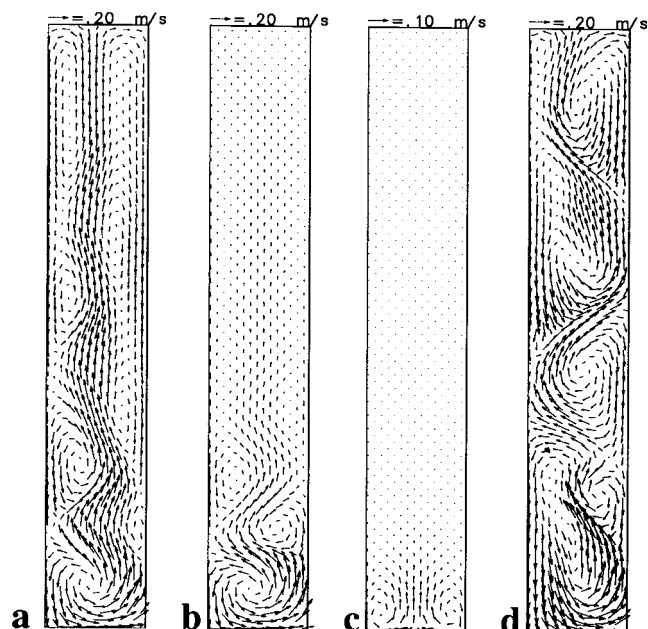


Figure 11. Time snapshot of liquid flow in the center vertical cross-section of a uniformly aerated bubble column for test cases a–d (s. Table 3).

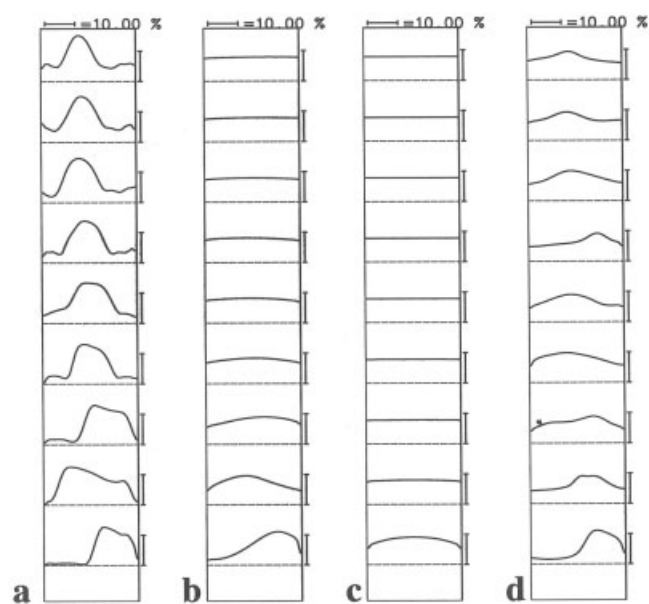


Figure 12. Time snapshot of gas profiles at different heights in the center vertical cross-section of a uniformly aerated bubble column for test cases a–d (s. Table 3).

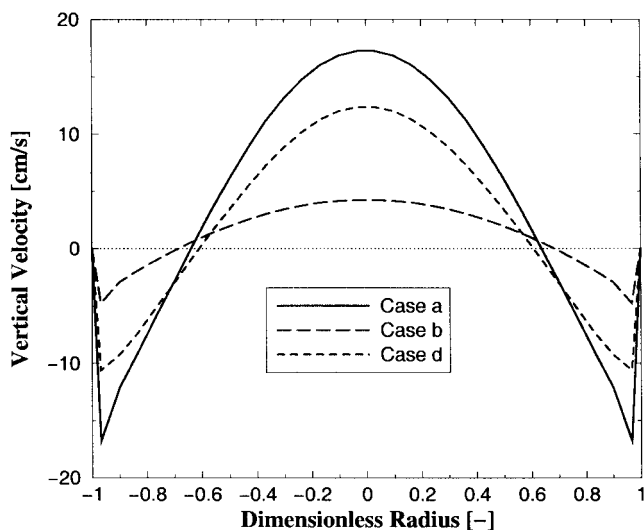


Figure 13. Long-time averaged liquid velocity profile at the half height of a uniformly aerated bubble column for test cases a, b and d (s. Table 3).

dispersion, which leads to almost flat gas holdup profiles in the middle and upper part of the column (Figure 12b). As a result, the liquid velocity maximum in the column center decreases from 17.2 cm/s to 4.2 cm/s (Figure 13). If bubble induced turbulence according to Kataoka and Serizawa (1989) with the same BIT-parameters as in Figure 10 ($C_k = 1$, $C_\varepsilon = 1.2$) is used, the turbulent viscosity in the column center rises from about $\mu_t^{\text{turb}} = 1.5$ to 3.8 [kg/m · s] and the resulting increase of turbulent gas dispersion leads to a completely stationary flow profile (Figures 11c and 12c).

In this case—contrary to the flat bubble column of Figure 10—the bubbles should therefore have a dampening effect on the turbulent viscosity. This can be modeled if a BIT-parameter of $C_\varepsilon = 1.92$, as in the work of Pflieger and Becker (2001), is used in Eq. 55. The turbulent viscosity now decreases to about $\mu_t^{\text{turb}} \approx 0.3$ [kg/m · s]. In spite of the fact that the gas holdup profiles (Figure 12d) are considerably flatter than in Case a, the reduced turbulent viscosity results in strongly dynamic flow profiles which extend over the total height of the column and agree well with visual observations (Figure 11d). Figure 13 shows that the maximum of the column center velocity now decreases from 1.72 cm/s (Case a) to 12.3 cm/s (Case d).

The examples show that different sets of model assumptions and model parameters may result in dynamic flow structures with similar long-time averaged velocity profiles. The detailed dynamic flow structures, however, can be remarkably different. This was already demonstrated by Sokolichin et al. (1997), who showed, for a uniformly aerated flat bubble column, that strongly different dynamic flow patterns may result in quantitatively similar long-time averaged flow profiles. This limits the use of long-time averaged flow profiles for the validation of bubble flow models.

As a consequence, it can be stated that the proper modeling of turbulent viscosity and turbulent bubble dispersion in bubbly flows requires more detailed experimental and theoretical attention. Experimentally, hardly any detailed information for uniformly aerated bubble columns, which can be used for turbulence model validation, is presently available. Since hy-

drodynamics in these bubble columns is both in stationary and turbulent, velocity fluctuations result both from local turbulence and from medium- and large-scale vortices. Appropriate models should, therefore, consist of a large-eddy-simulation approach, where the statistical turbulence model accounts for the short-time averaged velocity fluctuations, while the large eddies are resolved by the simulation. This requires that, experimentally, a separation between the short-time turbulent fluctuations and the fluctuations caused by larger-scale vortices also has to be made. Presently, most experimental results determine fluctuations only around the long-time average velocity. They can, therefore, not be used for turbulence model validation since the respective values of turbulent kinetic energy differ by almost one order of magnitude (Mudde et al., 1997). Only recently, some attempts have been made to look deeper into the structure of the liquid flow field (Mudde and van den Akker, 1999; Kulkarni et al., 2001).

Conclusions

In all cases where a flow is caused by the injection of gas bubbles into a liquid, the main flow driving force results from local density differences of the gas-liquid mixture, that is differences in the local gas holdup. Like any buoyancy driven flow, such a flow situation is highly unstationary and characterized by a spectrum of fluctuating vortices of different size. Its mathematical representation, therefore, requires to take the full 3-D, dynamic model equations into account.

The numerical solution of these detailed model equations, however, requires such a computational effort that up to now the detailed simulation and model-based design of gas-liquid reactors with bubbly flow like bubble columns or bubble column loop reactors has been severely impeded. It is, therefore, of prime importance to reduce the computational effort by reasonable simplifications of the hydrodynamics model.

In this contribution we discussed the two-fluid continuum approach where each volume element contains a mixture of gas and liquid, the mean density of which varies from element to element. Like in other buoyancy driven flows, the Boussinesq approximation for the momentum balance of the gas/liquid mixture proves to be reasonable. The mixture density changes are then neglected in all momentum terms and only considered in the buoyancy term. In addition any displacement of liquid by gas was neglected in the liquid continuity equation. The resulting model for the hydrodynamics of the gas/liquid mixture is similar to a single-phase flow model and can be solved efficiently with the respective well established iterative solution procedure. The validity of these simplifications has been proved for several examples by comparison with detailed simulation results.

In the above solution procedure the change of the local gas holdup has to be described by the solution of the gas-phase continuity and momentum equations. The latter requires the specification of the interaction forces between gas and liquid. Starting from the rise velocity of single bubbles, the pressure force and the drag force have been identified as most important. The added mass force proved to be negligible since the steady-state rising velocity for normal size bubbles in water is established within milliseconds. For the different lift forces, the literature provides only contradictory results. For buoyancy driven bubbly flow,

lift forces have so far been used primarily to adjust steady-state, 2-D simulation results to experiments. Since 3-D, dynamic simulations did not require an adjustment through additional lift forces, it is concluded that they are not essential for the simulation of the buoyancy driven bubbly flow. Since they are able to change the flow structure substantially, they should be omitted, as long as no clear experimental evidence of their direction and magnitude is available.

Many different correlations of rising bubbles exist. For the best studied system, air in water, most correlations agree with the experimental observation that, for bubble diameters between 2 and 8 mm, the bubble slip velocity is fairly constant. Since, in addition, the resulting flow structure is not very sensitive to the slip velocity, a constant slip velocity of about 25 cm/s proves to be a reasonable approximation for air/water bubbly flow. The favorable experimental evidence of almost constant slip velocity also is a liberation from the necessity to take bubble coalescence or dispersion into account as long as we stay in the homogeneous flow regime and no large bubbles as in churn turbulent flow are formed, and if only the flow pattern is of interest.

In the examples considered, dispersion of two different origins plays a crucial role. One cause of dispersion results from the numerical discretization of spatial gradients. Of particular concern are the convection terms in the continuity and momentum balances, if they are discretized with a common first-order upwind scheme. An (almost) dispersion free TVD discretization has to be used instead to prevent artificial numerical dispersion.

Contrary to the unwanted (while physically not justified) numerical dispersion, some physical dispersion of gas and liquid is brought about by the small-scale turbulent vortices. Since these vortices are too small to be simulated by the two-fluid approach, their influence has to be modeled by a turbulent diffusion mechanism. Simulation results show that the degree of diffusion of bubble plumes is essential for the resulting flow structure. This is again a characteristic consequence of the buoyancy driven flow.

Since bubble path diffusion is related to the turbulence, this leads to the important question of how turbulence in bubbly flows should be modeled. Presently, this remains the main open question in gas/liquid bubbly flow modeling. In cases when only a smaller part of the column was aerated, the standard k - ϵ -model for the liquid phase led to surprisingly good agreement between simulation and experiment. For more uniformly aerated systems, however, an additional turbulence effect of the rising bubbles is obvious. Several models for such a bubble induced turbulence have been proposed, but their model parameters so far seem not to possess much predictive power. Fundamental research, therefore, has to focus on the question of how bubbles in a swarm interact and change the turbulent energy generation and dissipation, as well as the bubble dispersion. Direct numerical simulation (DNS) of a flow of bubble clusters using continuum equations (Tryggvason et al., 1998) or a lattice Boltzmann approach (Shan and Chen, 1993) in combination with detailed flow visualization experiments which simultaneously show the dynamics of bubbles and the surrounding liquid (Borchers, 2002) are required to develop reliable models on this detailed level. After verification, they can be used to provide a well based description of the turbulent interaction phenomena, presently missing in the volume averaging two-fluid models.

In the meantime some caution concerning the predictive power of two-fluid models in the concentrated bubble flow regime is certainly justified.

Acknowledgments

Support of this work through Deutsche Forschungsgemeinschaft in the Schwerpunktprogramm "Analyse, Modellierung und Berechnung mehrphasiger Strömungen" is gratefully acknowledged. The authors are also grateful to Dr. Dmitri Kuzmin for fruitful discussions and valuable feedback.

Notation

- C_{am} = added mass coefficient, dimensionless
- C_d = drag coefficient, dimensionless
- C_k, C_ϵ = model coefficients for bubble induced turbulence, dimensionless
- C_l = life coefficient, dimensionless
- C_w = model coefficient, $C_w = 5 \times 10^4 \text{ kg/m}^3 \cdot \text{s}$
- d = diameter, m
- \mathbf{D}^{turb} = turbulent diffusion tensor, m^2/s
- $E\ddot{o}$ = Eötvös number, dimensionless, $E\ddot{o} = g\rho_l d_b^2/\sigma$
- \mathbf{F}_{int} = interphase force, N/m^3
- g = gravitational constant, 9.81 m/s^2
- k = turbulent kinetic energy, m^2/s^2
- m = mass, kg
- Mo = Morton number, dimensionless, $Mo = g\mu_l^4/\rho_l\sigma^3$
- p = pressure, N/m^2
- Re = Reynolds number, dimensionless, $Re = \rho_l d_b |\mathbf{u}_b - \mathbf{u}_l|/\mu_l$
- S_k, S_ϵ = additional source terms in k - or ϵ -equation
- Sc = Schmidt number, dimensionless
- t = time, s
- \mathbf{T}^{turb} = turbulent stress tensor, N/m^2
- V_b = volume, m^3
- \mathbf{u} = velocity vector, m/s
- We = Weber number, dimensionless, $We = \rho_l |\mathbf{u}_b - \mathbf{u}_l|^2 d_b/\sigma$

Greek Letters

- ϵ = dissipation rate of turbulent kinetic energy, m^2/s^2
- ϵ = holdup, dimensionless
- μ^{turb} = turbulent eddy viscosity, $\text{kg}/(\text{ms})$
- ∇ = gradient operator [$= (\partial/\partial x, \partial/\partial y, \partial/\partial z)$]
- ρ = density, kg/m^3
- σ = surface tension, kg/s^2

Sub- or Superscripts

- am = added mass
- b = bubble
- BI = bubble-induced
- d = drag
- g = gas phase or gravity
- k = gas or liquid phase
- l = liquid phase or lift
- p = pressure
- SI = shear-induced

Literature Cited

- Arnold, G. S., D. A. Drew, and R. T. Lahey, Jr., "Derivation of Constitutive Equations for Interfacial Force and Reynolds Stress for a Suspension of Spheres using Ensemble Averaging," *J. of Chem. Eng. Comm.*, **86**, 43 (1988).
- Auton, T. R., "The Lift Force on a Spherical Body in a Rotational Flow," *J. Fluid Mech.*, **183**, 199 (1987).
- Banerjee, S., "Modelling Considerations for Turbulent Multiphase Flows," *Engineering Turbulence Modelling and Experiments*, W. Rodi and E. N. Ganic, eds., Elsevier, New York, p. 831 (1990).
- Bauer, M., and G. Eigenberger, "Multiscale Modeling of Hydrodynamics,

- Mass Transfer and Reaction in Bubble Column Reactors," *Chem. Eng. Sci.*, **56**, 1067 (2001).
- Becker, S., A. Sokolichin, and G. Eigenberger, "Gas-Liquid Flow in Bubble Columns and Loop Reactors: II. Comparison of Detailed Experiments and Flow Simulations," *Chem. Eng. Sci.*, **49**, 5747 (1994).
- Bhanu, C., and D. Mazumdar, "Numerical Prediction of Melting Rates in Gas Bubble Driven Systems," *Trans. Indian. Inst. Met.*, **50**, 249 (1997).
- Boisson, N., and M. R. Malin, "Numerical Prediction of Two-Phase Flow in Bubble Columns," *Int. J. Num. Meth. Fluids*, **23**, 1289 (1996).
- Borchers, O., C. Busch, A. Sokolichin, and G. Eigenberger, "Applicability of the Standard $k-\epsilon$ Turbulence Model to the Dynamic Simulation of Bubble Columns: Comparison of Detailed Experiments and Flow Simulations," *Chem. Eng. Sci.*, **54**, 5927 (1999).
- Borchers, O., *Zweiphasen-Particle-Tracking-Velocimetry (PTV) zur Detaillierten Analyse der Hydrodynamik von Blasensäulenreaktoren*, VDI-Forstschrittberichte, Reihe 3: Verfahrenstechnik, Nr. 753. Düsseldorf: VDI-Verlag (2002).
- Boussinesq, J. V., *Theorie de l'écoulement Tourbillant*, Mem. Pres. Acad. Sci., Paris (1877).
- Boussinesq, J., *Theorie, Analytic de la Chaleur*, Gauthier-Villars, Paris (1903).
- Chen, R. C., J. Reese, and L.-S. Fan, "Flow Structure in a Three-Dimensional Bubble Column and Three-Phase Fluidized Bed," *AIChE J.*, **40**, 1093 (1994).
- Clift, R., J. R. Grace, and M. E. Weber, *Bubbles, Drops and Particles*, Academic Press, New York (1978).
- Deckwer, W.-D., *Bubble Column Reactors*, Wiley, Chichester (1992).
- Delnoij, E., F. A. Lammers, J. A. M. Kuipers, and W. P. M. van Swaaij, "Dynamic Simulation of Dispersed Gas-Liquid Two-Phase Flow using a Discrete Bubble Model," *Chem. Eng. Sci.*, **52**, 1429 (1997a).
- Delnoij, E., J. A. M. Kuipers, and W. P. M. van Swaaij, "Dynamic Simulation of Gas-Liquid Two-Phase Flow: Effect of Column Aspect Ratio on the Flow Structure," *Chem. Eng. Sci.*, **52**, 3759 (1997b).
- Delnoij, E., J. A. M. Kuipers, and W. P. M. van Swaaij, "A Three-Dimensional CFD Model for Gas-Liquid Bubble Columns," *Chem. Eng. Sci.*, **54**, 2217 (1999).
- Deng, H., R. K. Mehta, and G. W. Warren, "Numerical Modeling of Flows in Flotation Columns," *Int. J. Miner. Process.*, **48**, 61 (1996).
- Devanathan, N., M. P. Dudukovic, A. Lapin, and A. Lübbert, "Chaotic Flow in Bubble Column Reactors," *Chem. Eng. Sci.*, **50**, 2661 (1995).
- Djebbar, R., M. Roustan, and A. Line, "Numerical Computation of Turbulent Gas-Liquid Dispersion in Mechanically Agitated Vessels," *Trans. IChemE*, **74 Part A**, 492 (1996).
- Drew, D. A., "Mathematical Modeling of Two-Phase Flow," *Ann. Rev. Fluid Mech.*, **15**, 261 (1983).
- Elghobashi, S. E., and T. W. Abou-Arab, "A Two-Equation Turbulence Model for Two-Phase Flows," *Phys. Fluids*, **26**, 931 (1983).
- Esmaeeli, A., E. Ervin, and G. Tryggvason, "Numerical Simulations of Rising Bubbles," *Bubble Dynamics and Interface Phenomena*, J. R. Blake, ed.; Kluwer Academic, Dordrecht, The Netherlands (1994).
- Fan, L.-S., and K. Tsuchiya, *Bubble Wake Dynamics in Liquids and Liquid-Solid Suspensions*, Butterworth-Heinemann, Boston (1990).
- Ferziger, J. H., and M. Peric, *Computational Methods for Fluid Dynamics*, Springer, Berlin (1996).
- Grienberger, J., and H. Hofmann, "Investigations and Modelling of Bubble Columns," *Chem. Eng. Sci.*, **47**, 2215 (1992).
- Grienberger, J., "Untersuchung und Modellierung von Blasensäulen," PhD Thesis, Universität Erlangen-Nürnberg (1992).
- Haberman, W. L., and R. K. Morton, "An Experimental Investigation of the Drag and Shape of Air Bubbles Rising in Various Liquids," David W. Taylor Model Basin Report 802, U.S. Navy Dept., Washington, DC (1953).
- Hillmer, G., L. Weismantel, and H. Hofmann, "Investigations and Modelling of Slurry Bubble Columns," *Chem. Eng. Sci.*, **49**, 837 (1994).
- Hills, J. H., "Radial Non-Uniformity of Velocity and Voidage in a Bubble Column," *Trans. Instn. Chem. Engrs.*, **52**, 1 (1974).
- Hsieh, D. Y., "On Dynamics of Bubbly Liquids," *Adv. in Appl. Mech.*, **26**, 63 (1988).
- Ilgbusi, O. J., M. Iguchi, K. Nakajima, S. Mitsuhiro, and M. Sakamoto, "Modeling Mean Flow and Turbulence Characteristics in Gas-Agitated Bath with Top Layer," *Metallurgical and Materials Trans. B.*, **29B**, 211 (1998).
- Ishii, M., *Thermo-Fluid Dynamic Theory of Two-Phase Flow*, Eyrolles, Paris (1975).
- Ishii, M., and N. Zuber, "Drag Coefficient and Relative Velocity in Bubbly, Droplet or Particulate Flows," *AIChE J.*, **25**, 843 (1979).
- Jakobsen, H. A., B. H. Sannaes, S. Grevskott, and H. F. Svendsen, "Modeling of Vertical Bubble-Driven Flows," *Ind. Eng. Chem. Res.*, **36**, 4052 (1997).
- Jenne, M., *Modellierung und Simulation der Strömungsverhältnisse in begasten Rührkesselreaktoren*, MVK-Verlag, Tübingen (1999).
- Johansen, S. T., and F. Boysan, "Fluid Dynamics in Bubble Stirred Ladles: II. Mathematical Modeling," *Metallurgical Trans. B.*, **19B**, 755 (1988).
- Joshi, J. B., "Computational Flow Modelling and Design of Bubble Column Reactors," *Chem. Eng. Sci.*, **56**, 5893 (2001).
- Joshi, J. B., V. S. Vitankar, A. A. Kulkarni, M. T. Dhotre, and K. Ekambara, "Coherent Flow Structures in Bubble Column Reactors," *Chem. Eng. Sci.*, **57**, 3157 (2002).
- Kataoka, I., and A. Serizawa, "Basic Equations of Turbulence in Gas-Liquid Two-Phase Flow," *Int. J. Multiphase Flow*, **15**, 843 (1989).
- Krishna, R., J. M. van Baten, and M. I. Urseanu, "Three-Phase Eulerian Simulations of Bubble Column Reactors in the Churn-Turbulent Regime. A Scale-Up Strategy," *Chem. Eng. Sci.*, **55**, 3275 (2000).
- Kulkarni, A. A., J. B. Joshi, and V. R. Kumar, "Identification of the Principal Time Scales in Bubble Column by Wavelet Analysis," *Chem. Eng. Sci.*, **56**, 5739 (2001).
- Kuo, J. T., and G. B. Wallis, "Flow of Bubbles through Nozzles," *Int. J. Multiphase Flow*, **14**, 547 (1988).
- Kuo, T. C., C. Pan, C. C. Chieng, and A. S. Yang, "Eulerian-Lagrangian Computations on Phase Distribution of Two-Phase Bubbly Flows," *Int. J. Num. Meth. Fluids*, **24**, 579 (1997).
- Kuwagi, K., and H. Ozoe, "Three-Dimensional Oscillation of Bubbly Flow in a Vertical Cylinder," *Int. J. Multiphase Flow*, **25**, 175 (1999).
- Kuzmin, D., "Numerical Simulations of Reactive Bubbly Flows," PhD Thesis, University of Jyväskylä, Jyväskylä, Finland (1999).
- Lahey, Jr., R. T., "The Analysis of Phase Separation and Phase Distribution Phenomena using Two-Fluid Models," *Nucl. Eng. Des.*, **122**, 17 (1990).
- Lain, S., D. Bröder, and M. Sommerfeld, "Experimental and Numerical Studies of the Hydrodynamics in a Bubble Column," *Chem. Eng. Sci.*, **54**, 4913 (1999).
- Lapin, A., C. Maul, K. Junghans, and A. Lübbert, "Industrial-Scale Bubble Column Reactors: Gas-Liquid Flow and Chemical Reaction," *Chem. Eng. Sci.*, **56**, 239 (2001).
- Lin, T.-J., J. Reese, T. Hong, and L.-S. Fan, "Quantitative Analysis and Computation of Two-Dimensional Bubble Columns," *AIChE J.*, **42**, 301 (1996).
- Liu, T. J., "Experimental Investigation of Turbulence Structure in Two-Phase Bubbly Flow," PhD Thesis, Northwest University (1989).
- Lopez de Bertodano, M., R. T. Lahey, Jr., and O. C. Jones, "Development of a $k-\epsilon$ Model for Bubbly Two-Phase Flow," *Trans. of ASME*, **116**, 128 (1994a).
- Lopez de Bertodano, M., R. T. Lahey, Jr., and O. C. Jones, "Phase Distribution in Bubbly Two-Phase Flow in Vertical Ducts," *Int. J. Multiphase Flow*, **20**, 805 (1994b).
- Morud, K. E., "Turbulent Two-Phase Flow in Bubble Columns and Stirred Fermenters," Dr. Ing. Thesis, NTH, TMH, Porsgrunn, Norway (1994).
- Morud, K. E., and B. H. Hjertager, "LDA Measurements and CFD Modelling of Gas-Liquid Flow in a Stirred Vessel," *Chem. Eng. Sci.*, **51**, 233 (1996).
- Mudde, R. F., D. J. Lee, J. Reese, and L.-S. Fan, "Role of Coherent Structures on Reynolds Stresses in a 2-D Bubble Column," *AIChE J.*, **43**, 913 (1997).
- Mudde, R. F., and O. Simonin, "Two- and Three-Dimensional Simulations of a Bubble Plume Using a Two-Fluid Model," *Chem. Eng. Sci.*, **54**, 5061 (1999).
- Mudde, R. F., and H. E. A. van den Akker, "Dynamic Behavior of the Flow Field of a Bubble Column at Low to Moderate Gas Fractions," *Chem. Eng. Sci.*, **54**, 4921 (1999).
- Murai, Y., and Y. Matsumoto, "Numerical Analysis of Detailed Flow Structures of a Bubble Plume," *JSME Int. J. Ser. B*, **41**, 568 (1998).
- Pan, S.-M., Y.-H. Ho, and W.-S. Hwang, "Three-Dimensional Fluid Flow Model for Gas-Stirred Ladles," *J. of Materials Eng. and Performance (JMEPEG)*, **6**, 311 (1997).
- Pan, Y., M. P. Dudukovic, and M. Chang, "Dynamic Simulation of Bubbly Flow in Bubble Columns," *Chem. Eng. Sci.*, **54**, 2481 (1999).
- Pan, Y., M. P. Dudukovic, and M. Chang, "Numerical Investigation of Gas-Driven Flow in 2-D Bubble Columns," *AIChE J.*, **46**, 434 (2000).
- Park, H.-J., and W.-J. Yang, "Turbulent Two-Phase Mixing in Gas-Stirred

- Ladle Systems for Continuous Casting Applications," *Numerical Heat Transfer, Part A*, **31**, 493 (1997).
- Patankar, S. V., *Numerical Heat Transfer and Fluid Flow*, McGraw-Hill, New York (1980).
- Pfleger, D., and S. Becker, "Modelling and Simulation of the Dynamic Flow Behavior in a Bubble Column," *Chem. Eng. Sci.*, **56**, 1737 (2001).
- Ranade, V. V., and H. E. A. van den Akker, "A Computational Snapshot of Gas-Liquid Flow in Baffled Stirred Reactors," *Chem. Eng. Sci.*, **49**, 5175 (1994).
- Richardson, J. R., and W. N. Zaki, "Sedimentation and Fluidization: I," *Trans. Inst. Chem. Eng.*, **32**, 35 (1954).
- Sanyal, J., S. Vasquez, S. Roy, and M. P. Dudukovic, "Numerical Simulation of Gas-Liquid Dynamics in Cylindrical Bubble Column Reactors," *Chem. Eng. Sci.*, **54**, 5071 (1999).
- Sato, Y., and K. Sekoguchi, "Liquid Velocity Distribution in Two-Phase Bubble Flow," *Int. J. Multiphase Flow*, **2**, 79 (1975).
- Sato, Y., M. Sadatomi, and K. Sekoguchi, "Momentum and Heat Transfer in Two-Phase Bubble Flow," *Int. J. Multiphase Flow*, **7**, 167 (1981).
- Schlueter, M., and N. Raebiger, "Bubble Swarm Velocity in Two-Phase Flows," *HTD-Vol. 361, Proc. of ASME Heat Transfer Division*, Volume 5, ASME, New York (1998).
- Schwarz, M. P., and W. J. Turner, "Applicability of the Standard $k-\epsilon$ Turbulence Model to Gas-Stirred Baths," *Appl. Math. Modelling*, **12**, 273 (1988).
- Serizawa, A., *Fluid-Dynamic Characteristics of Two-Phase Flow*, PhD Thesis, Kyoto University (1974).
- Serizawa, A., I. Kataoka, and I. Michiyoshi, "Phase Distribution in Bubbly Flow," *Proc. Int. Workshop on Two-Phase Flow Fundamentals*, Data Set No. 24 (1986).
- Shan, X., and H. Chen, "Lattice Boltzmann Model for Simulating Flows with Multiple Phases and Components," *Physical Rev. E*, **47**, 1815 (1993).
- Simonin, O., and P. Violet, "Modelling of Turbulent Two-Phase Jets Loaded with Discrete Particles," *Phenomena in Multiphase Flow*, F. G. Hewitt, et al., eds., Hemisphere, Washington, DC, pp. 259–269 (1990).
- Sokolichin, A., and G. Eigenberger, "Gas-Liquid Flow in Bubble Columns and Loop Reactors: Part I. Detailed Modeling and Numerical Simulation," *Chem. Eng. Sci.*, **49**, 5735 (1994).
- Sokolichin, A., G. Eigenberger, A. Lapin, and A. Lübbert, "Dynamic Numerical Simulation of Gas-Liquid Two-Phase Flows: Euler-Euler Versus Euler-Lagrange," *Chem. Eng. Sci.*, **52**, 611 (1997).
- Sokolichin, A., and G. Eigenberger, "Applicability of the Standard $k-\epsilon$ Turbulence Model to the Dynamic Simulation of Bubble Columns: Part I. Detailed Numerical Simulations," *Chem. Eng. Sci.*, **54**, 2273 (1999).
- Sommerfeld, M., S. Decker, and G. Kohnen, "Time-Dependent Calculation of Bubble Columns Based on Reynolds-Averaged Navier-Stokes Equations with $k-\epsilon$ Turbulence Model," *Proc. of the 2nd Japanese-German Symp. on Multi-Phase Flow*, Tokyo, Paper No. 3-1-4, 323 (1997).
- Smith, B. L., and M. Milelli, "An Investigation of Confined Bubble Plumes," *Proc. of Third Int. Conf. Multiphase Flow*, ICMF 1998, Lyon, France (Jun. 8–12, 1998).
- Spalding, D. B., "The Calculation of Free-Convection Phenomena in Gas-Liquid Mixtures," Imperial College, HTS No. 76, London (1976).
- Spalding, D. B., "Computer Simulation of Two-Phase Flows with Special Reference to Nuclear Reactor Systems," *Computational Techniques in Heat Transfer*, R. W. Lewis, ed., Pineridge Press, Swansea, U.K., p. 1 (1985).
- Stone, H. L., "Iterative Solution of Implicit Approximations of Multidimensional Partial Differential Equations," *SIAM J. Numer. Anal.*, **5**, 530 (1968).
- Svendsen, H. F., H. A. Jakobsen, and R. Torvik, "Local Flow Structures in Internal Loop and Bubble Column Reactors," *Chem. Eng. Sci.*, **47**, 3297 (1992).
- Thomas, N. H., T. R. Auton, K. Sene, and J. C. R. Hunt, "Entrapment and Transport of Bubbles in Transient Large Eddies in Multiphase Turbulent Shear Flows," *Int. Conf. on Physical Modelling of Multi-Phase Flows*, Coventry, U.K. 169 (1983).
- Tomiya, A., I. Kataoka, and T. Sakaguchi, "Drag Coefficients of Bubbles, 1st Report: Drag Coefficient of a Single Bubble in a Stagnant Liquid," (in Japanese), *Trans. JSME, Ser. B.*, **61**, 2357 (1995a).
- Tomiya, A., A. Sou, I. Zun, N. Kanami, and T. Sakaguchi, "Effect of Eötvös Number and Dimensionless Liquid Volumetric Flux on Lateral Motion of a Bubble in a Laminar Duct Flow," *Proc. Int. Conf. Multiphase Flow*, Kyoto, PD1, 11 (1995b).
- Tomiya, A., "Struggle with Computational Bubble Dynamics," *Proc. of Third Int. Conf. Multiphase Flow*, ICMF 1998, Lyon, France (Jun. 8–12, 1998).
- Torvik, R., and H. F. Svendsen, "Modelling of Slurry Reactors: A Fundamental Approach," *Chem. Eng. Sci.*, **45**, 2325 (1990).
- Tryggvason, G., B. Bunner, A. Esmaeeli, and S. Mortazavi, "Direct Numerical Simulations of Dispersed Flows," *Proc. of Third Int. Conf. Multiphase Flow*, ICMF 1998, Lyon, France (Jun. 8–12, 1998).
- Tsuchiya, K., A. Furumoto, L.-S. Fan, and J. Zhang, "Suspension Viscosity and Bubble Rise Velocity in Liquid-Solid Fluidized Beds," *Chem. Eng. Sci.*, **52**, 3053 (1997).
- van den Akker, H. E. A., "Momentum Equations in Dispersed Two-Phase Flows," *Encyclopedia of Fluid Mechanics*, Vol. 3, Gulf Publishing, Houston, p. 371 (1986).
- Wang, S. K., S. J. Kee, O. C. Jones, Jr., and R. T. Lahey, Jr., "3-D Turbulence Structure and Phase Distribution Measurements in Bubbly Two-Phase Flows," *Int. J. Multiphase Flow*, **13**, 237 (1987).
- Wesselingh, J. A., "The Velocity of Particles, Drops and Bubbles," *Chem. Eng. Process*, **21**, 9 (1987).

Manuscript received Feb. 10, 2003, and revision received May 27, 2003.